The impacts of marine-emitted halogens on OH radicals in East Asia during summer

Shidong Fan[1,2], Ying Li[1,2,3]

[1]Department of Ocean Science and Engineering, Southern University of Science and Technology, Shenzhen 518055, China
[2]Center for the Oceanic and Atmospheric Science at SUSTech (COAST), Southern University of Science and Technology, Shenzhen 518055, China
[3]Southern Marine Science and Engineering Guangdong Laboratory (Guangzhou) China

Correspondence to: Ying Li (liy66@sustech.edu.cn)

Abstract. Relationships between oceanic emissions and air chemistry are intricate and still not fully understood. For regional air chemistry, a better understanding of marine halogen emission on ~~Hydroxyl~~ hydroxyl (OH) radical is crucial. The OH radical is a key species in atmospheric chemistry because it can oxidize almost all trace species in the atmosphere. In the marine atmosphere, OH levels could be significantly affected by the halogen species emitted from the ocean. However, due to the complicated interactions of halogens with OH through different pathways, it is not well understood how halogens influence OH and even what the sign of the net effect is. Therefore, in this study, we aim to quantify the impact of marine-emitted halogens (including Cl, Br, and I) through different pathways on OH in the high OH season by using WRF-CMAQ model with process analysis and state-of-the-art halogen chemistry in the East Asia ~~Seas.~~and near western pacific. Results show a very complicated response of the OH production rate (P_{OH}) to marine halogen emissions. The monthly P_{OH} is generally decreased over the ocean by up to a maximum of about 10–15% in the Philippine Sea, but is increased in many nearshore areas by up to about 7–9% in the Bohai Sea. In the coastal areas of southern China, the monthly P_{OH} could also decrease 3–5% in the Greater Bay Area, but ~~with a daytime~~ hourly ~~maximum~~values can decrease over 30% in the daytime. Analysis of the individual reactions using integrated reaction rate (IRR) show that the net change of P_{OH} is controlled by the competitions of three main pathways (OH from O_3 photolysis, OH from HO_2 conversion, and OH from HOX, X=Cl, Br, I) through different halogen species. Sea spray aerosols (SSA) and inorganic iodine gases are the ~~main~~major species to influence the strengths of these three pathways and therefore have the most significant impacts on P_{OH}. Both of these two types of species decrease P_{OH} through physical processes, while generally ~~increase~~ increasing P_{OH} through chemical processes. In the ocean atmosphere, ~~the controlling species are~~ inorganic iodine gases ~~and the~~ determine the basic pattern of ΔP_{OH} through complicated iodine chemistry ~~determines the basic pattern of ΔP_{OH},~~which generally positively influences P_{OH} near O_3 sources while negatively when O_3 experiences longer transport over the ocean. Over the continent, SSA is the controlling species and the SSA extinction effect leads to the negative ΔP_{OH} in ~~the~~ southern China. Our results ~~indicate~~show that marine-emitted halogen species have notable impacts over the ocean and ~~have~~ potential impact on ~~the~~ coastal atmospheric oxidation~~. The identified~~ by species (SSA, inorganic iodine, and halocarbons), processes (chemistry, radiation,

and deposition) and main ~~(previously known or unknown)~~ pathways ~~and their controlling factors from different~~. The notable impacts of the marine-emitted halogen species ~~to OH radical explains the halogen-induced change of P_{OH}~~on the atmospheric oxidation capacity have further implications in the lifetime of long-lived species such as CH_4 in long-term and amount of air pollutants such as O_3 in the episodic events in East Asia and ~~also can be applied~~ in other circumstances (e.g., different domains, regions, and emission rates).

1 Introduction

The h~~H~~ydroxyl radical is the most important daytime oxidant in the troposphere. It can oxidize almost all directly emitted gases such as CO, CH_4 and other volatile organic compounds (VOCs), while ~~produce~~ producing some secondary species such as O_3 and secondary aerosols at the same time. The ~~dominant sources~~primary source of OH ~~are HO_2 and O_3 over~~in the ~~continental areas~~troposphere is O_3, through the reaction of ~~HO_2~~water vapor with ~~NO and~~$O(^1D)$ which is produced from the photolysis of O_3 ~~and following reaction of O^1D with water vapor, respectively~~. At urban areas, the photolysis of HONO is also a significant source of OH, and may be more important than the photolysis of O_3, especially in spring, autumn, and winter because of the very large seasonal ~~variation~~variations of O_3 photolysis and humidity (e.g., Tan et al., 2019;Whalley et al., 2021;Liu et al., 2019). ~~The main sinks of OH are CO and VOCs. Recently, studies showed that in the low-NO*x* conditions, OH modeled by current chemical mechanisms are usually underestimated~~When there is abundant NO, as typically in the polluted continental atmosphere, peroxy radicals (RO_2 and HO_2) will be formed by the oxidation of hydrocarbons by OH, and will form OH again in the reaction with NO. This HO*x* (=OH+HO_2) cycling maintains a high OH concentration that cannot be achieved by primary sources alone. The main sinks of OH are CO and VOCs. Due to the complexity of the HO*x* chemistry, the sources and sinks of OH are not fully understood. For example, recent studies showed that when NO*x* concentration is very low there may be missing sources of OH. (Tan et al., 2019;Rohrer et al., 2014;Lelieveld et al., 2008;Hofzumahaus et al., 2009;Lu et al., 2019a;Fuchs et al., 2013;Stone et al., 2012;Fittschen et al., 2019;Whalley et al., 2021)~~, and missing sources of OH is a common hypothesis. To account for such a missing source of OH, efforts have been made to update RO_2 chemistry, by introducing artificial pathways first and mechanistic pathways later that convert RO_2 to OH (e.g., Bates and Jacob, 2019;Archibald et al., 2010). However, due to the complexity of RO_2 chemistry, current understanding on the missing source of OH in the low-NO*x* condition is still open.~~. Besides, HO*x* chemistry can interact with other oxidizers in the atmosphere in specific circumstances.

In the marine atmosphere, the abundant marine-emitted halogen species have significant impacts on OH. ~~The marine~~Marine-emitted halogen could make the tropospheric HO*x*-NO*x*-O_3-VOCs chemistry more complex. ~~One relevant reaction is that XO (X=Cl, Br, and I) transform HO_2 to OH, as NO does in the high-NO*x* condition. As a consequence, previous box-model studies usually showed positive impacts of halogen chemistry on OH (Stone et al., 2018;Whalley et al., 2010). However, there is an opposite impact of halogens on OH as usually shown by chemical transport model (CTM) studies that halogen~~

~~species will consume O_3 which in turn would reduce the production of OH~~ One relevant reaction is that XO (X=Cl, Br, and I) shifts the HO*x* balance towards OH (Saiz-Lopez and von Glasow, 2012). As a consequence, previous box-model studies usually showed positive impacts of halogen chemistry on OH (Stone et al., 2018;Whalley et al., 2010)~~. In box-model studies, long-term species such as O_3 are usually observation constrained and cannot reflect the influence of halogens, probably resulting the difference between box models and CTMs (Stone et al., 2018). Therefore, special attention needs to be paid when using box models to quantify the complicated impacts of halogen species on the HO*x*-NO*x*-O_3-VOCs chemistry. In CTMs studies, the two pathways (i.e., enhanced HO_2 conversion by XO and O_3 consumption by X atoms) are well described, but it is not very clear which process will dominate. Furthermore, the impacts of halogen species on OH are actually more complex than the two pathways. First, there may be other important impacts of halogen on the sources or sinks of OH. For example, the conversion of HO_2 to OH enhanced by XO would consume HO_2, which in turn should decrease the conversion through HO_2+NO. Previous CTM studies generally did not consider such an impact (e.g., Stone et al., 2018). Besides, other sources of OH, including the photolysis of HONO and H_2O_2, ozonolysis of some alkene, and the decomposition of some fragmentation of the aromatic hydrocarbons, as well as the chemistry of peroxyl radicals could also be influenced by halogen chemistry. Second, different halogen species generally have different impacts on OH, indicating different controlling factors to the pathways for different halogen species, making the net impact of all halogen species variable. For example, Stone et al. (2018) showed iodine will generally increase OH while bromine the opposite, and their combined effect is more subtle. However, previous studies did not analyze the pathways themselves and it remains unclear what processes control the strengths of the known and unknown (if exist) pathways of different species and how these pathways interact. Moreover, since current estimations of marine halogen emissions have large uncertainties, the stability of the interaction result of different pathways may be subject to the uncertainties in the emission estimation and variation in controlling factors of the various pathways~~. However, there is an opposite impact of halogens on OH as usually shown by chemical transport model (CTM) studies that halogen species will consume O_3 which in turn would reduce the production of OH (e.g., Sherwen et al., 2016;Stone et al., 2018). For example, Wang et al. (2021) showed that the net effect of halogen chemistry on global tropospheric HO*x* is that both OH and HO_2 are reduced by 3–4%. In a box model, when the long-lived species such as O_3 are observation-constrained, it cannot reflect the complete influence of halogens, which probably result in the different results between box models and CTMs (Stone et al., 2018). Therefore, special attention needs to be paid when using box models to quantify the complicated impacts of halogen species on the HO*x*-NO*x*-O_3-VOCs chemistry.

~~In short, recent studies in understanding the impacts of halogen chemistry on OH usually focused on the two pre-described pathways (i.e., enhanced HO_2 conversion by XO and O_3 consumption by X atoms) which are not directly quantified.~~In additional to present the global impact quantitatively, a more comprehensive understanding on the changes by species (SSA, inorganic iodine, and halocarbons) and their associated processes (chemistry, radiation, and deposition) is needed in order to better explain relevant observed or modeled phenomena and their driving factors. However, the pathways and processes by which halogens influence OH have not been well quantified in previous studies. Recent studies in understanding the impacts of halogen chemistry on OH usually focused on the two pre-described pathways (i.e., enhanced HO_2 conversion by XO and

O_3 consumption by X atoms). Even though we know all the important pathways, due to their opposite impacts on OH, we need further to understand the controlling processes of these pathways in order to better explain the trend of halogen-induced ΔOH in a specific circumstance. Moreover, since current estimations of marine halogen emissions, including SSA Cl and Br ions (and their activations), inorganic iodine (I_2 and HOI), and very short-lived halocarbons), have large uncertainties (Carpenter et al., 2021;Ordóñez et al., 2012;Ziska et al., 2013;Inamdar et al., 2020;Lennartz et al., 2015;Zhu et al., 2019;Sekiya et al., 2020;Wang et al., 2021;Grythe et al., 2014), the stability of the interaction result of different pathways may be subject to the uncertainties in the emission estimation and variation in controlling factors of the various pathways. Therefore, in order to better understand the role of halogen chemistry on tropospheric OH, we explore the pathways by which halogen species influence OH, and how these pathways interact with each other and how they are influenced by different species-related processes in this study, based on current knowledge about halogen chemistry and marine emissions of halogen species. We ~~use~~carried out model simulations to quantify the contributions of different pathways by using a regional CTM (Community Multiscale Air Quality Modeling System, CMAQ) with process analysis (PA, including Integrated Process Rate, IPR, and Integrated Reaction Rate, IRR) ~~in a CTM (CMAQ) to separate different pathways. Furthermore, the~~over East Asia and Western Pacific during summer. The controlling factors of strengths of the different pathways, mainly represented by different species-related processes, are analyzed based on PA and relevant sensitivity simulations, and their interactions are discussed. With higher spatial resolution than global models, we also explore the interaction of anthropogenic emissions with marine halogen emissions when discussing the controlling factors of strengths of the different pathways in iodine chemistry. The emission uncertainties are taken into consideration by running sensitivity simulations using ~~extreme~~the largest or the smallest emission rates that have been used or reported in previous studies. The setup of the models and the estimations of marine emission and its extreme uncertainties of halogen species are described in Section 2. Results and discussions are in Section 3. Section 4 gives conclusions.

2. Methods

2.1 Model setup

We use the CMAQ model, driven by meteorological fields from Weather Research and Forecasting Model (WRF), to explore the impact of halogens on OH. For WRF (version 3.9.1), the domain has a horizontal resolution of 27km and the number of grids is 283×184. The vertical coordinates contain 39 sigma levels. The initial and boundary conditions are generated from the NCEP GDAS/FNL 0.25° analysis data. Analysis and observation nudging are applied. The data used for observation nudging are obtained from NCEP datasets *ds461.0* (for surface) and *ds361.1* (for upper layer). For major physical parameterizations, the Rapid Radiative Transfer Model (RRTM) longwave radiation scheme, the Dudhia shortwave radiation scheme, the WRF Single-Moment 3-class microphysics scheme, the Noah Land Surface Model, and the Grell-Freitas ensemble cumulus scheme are applied.

CMAQ (version 5.3.2) (Appel et al., 2021) has the same horizontal resolution as WRF, but with a slightly smaller domain. The vertical layers are the lowest 20 layers plus six of the remaining 19 layers of WRF. The chemical mechanism~~s~~ adopted here is CB6r3m released in CMAQv5.3, which is updated by adding halogen chemistry to CB6r3 mechanism based on the work of Sarwar and co-workers (Sarwar et al., 2019;Sarwar et al., 2015;Sarwar et al., 2014;Sarwar et al., 2012). Details of the gaseous reactions and heterogeneous reactions can be found in the recent work of Sarwar et al. (2019) and Sarwar et al. (2012) (see also Table S1). A Rosenbrock (ROS3) solver is used to solve the chemical reactions and the absolute and relative error tolerances are set to 10^{-9} ppm and 10^{-3}, respectively. The initial and boundary conditions for CMAQ are extracted from a seasonal average hemispheric CMAQ output file that is obtained from the CMAS data warehouse (https://github.com/USEPA/CMAQ/blob/master/DOCS/Users_Guide/Tutorials/CMAQ_UG_tutorial_HCMAQ_IC_BC.md, last access: 6 October 2021). This hemispheric CMAQ used the same chemical mechanism as ours. The anthropogenic emissions are from MEIC (http://www. meicmodel.org/), while the emissions in the Guangdong province are replaced by local emissions that are based on a local emission inventory (Yin et al., 2015;Zheng et al., 2009) and processed by the Sparse Matrix Operator Kernel Emissions (SMOKE) processor. No halogen species are contained in the anthropogenic emissions. The terrestrial biogenic emissions are processed by MEGAN2.1 (Guenther et al., 2012). Other routine configuration set up of the model can be referred to Fan et al. (2021).

Because OH concentration is highest in summer, the simulations of this study are for the month of July 2019, including an additional 10 day in June for spin-up following Li et al. (2020).

2.2 Marine emissions of halogen species

There are three main types of halogen species emitted from the ocean: SSA (Cl and Br), inorganic iodine (I_2 and HOI), and halocarbons including $CHBr_3$, CH_2Br_2, CH_2BrCl, $CHBr_2Cl$, $CHBrCl_2$, CH_3I, CH_2ICl, CH_2IBr, and CH_2I_2 (e.g., Sarwar et al., 2019;Carpenter et al., 2013;Ordóñez et al., 2012;Wang et al., 2019). The latest release version of CMAQ (v5.3) contains these emissions ~~inline~~online.

The SSA emission in current CMAQ is updated by Gantt et al. (2015) on the top of the work of Kelly et al. (2010). The source function is based on the widely used source function developed by Gong (2003) which is an update of Monahan et al. (1986). Two main changes were implemented by Gantt et al. (2015). One is to add an SST-correction function to the source function because SST has large impacts on SSA flux (e.g., Barthel et al., 2019;Liu et al., 2021). The other is to change the shape factor of the source function (which determines the shape of the flux distribution) to emit more submicron SSA (see Fig. S1 of Gantt et al. (2015)). The SST-correction function is based on the work of Ovadnevaite et al. (2014) and is linear. This is different from another widely used observation-based SST-correction function developed by Jaeglé et al. (2011) which is a 3-order function of SST, but at high temperature (~30°C) their values are close (see ~~Fig. S3 of the preprint version of Ovadnevaite et al. (2014)).~~eq. 2 of Gantt et al. (2015) and eq. 4 of Jaeglé et al. (2011)). Besides these two main changes, surf-enhanced emission is also reduced by narrowing the surf zone which was previously defined as 50 m to the coast and now reduced to 25 m as in the study of Gantt et al. (2015).

Inorganic iodine and halocarbons, as well as Br in SSA, are implemented as by Sarwar and co-workers (Sarwar et al., 2019). Inorganic iodine emissions are based on the work of Carpenter et al. (2013) which parameterized the emission of I_2 and HOI as functions of O_3 concentration, aqueous iodine concentration, and surface wind speed (see eqs. 19 and 20 in the SI of Carpenter et al. (2013)). Halocarbon emissions are calculated based on the work of Ordóñez et al. (2012) which directly related flux of halocarbons to chlorophyll-*a* (chl-*a*) concentration.

Current estimations of marine halogen emissions have large uncertainties. There are many different source functions of SSA, and the difference of the SSA flux calculated based on these source functions are very large (Grythe et al., 2014). The parameterizations of aqueous iodine have also different versions and differ largely (MacDonald et al., 2014;Sherwen et al., 2019;Chance et al., 2014). The halocarbon emissions are entirely empirical which have few physical bases. Therefore, it is necessary to consider the influence of the uncertainty in the emissions on final results. We design two simulation groups with different emission rates, one high and one low. The high and low emission rates are taken from previously used estimations, similar to the work of Sekiya et al. (2020). The low emission rate of SSA is calculated using the source function in Gong (2003) directly, while the high emission rate using the source function modified by Gantt et al. (2015) because adding SST-correction function is somewhat more important than using different source functions (Barthel et al., 2019) and the source function of Gong (2003) or its modifications are the most widely used one. The parameterizations of I_2 and HOI emissions are less variable and only that by Carpenter et al. (2013) is widely used. However, there are two widely used parameterizations of aqueous iodine with large difference. Therefore, the low emission rate of I_2 and HOI is calculated using low concentration of aqueous iodine, taking from MacDonald et al. (2014), while the high emission rate using high concentration, taking from Chance et al. (2014). ~~The calculation of halocarbon emissions are~~The calculation of halocarbon emissions, which is based on the estimation of Ordóñez et al. (2012), is constrained by global annual flux (Sarwar et al., 2015); therefore, we increase or decrease halocarbon emissions based on the ratios of global annual halocarbon fluxes reported by WMO (Engel et al., 2019) to that in Ordóñez et al. (2012)~~.~~Ordóñez et al. (2012). The scale factors are shown in Table S2. The chl-*a* data are obtained from the merged products of the GlobColour data set (http://globcolour.info, last access: 6 October 2021) that is developed, validated, and distributed by ACRI-ST, France.

The emissions of inorganic iodine are accompanied by the consumption of O_3 at the ocean surface~~, but current CTMs do not couple these two processes. Instead, an~~. An enhanced O_3 dry deposition by oceanic iodine is usually added (Luhar et al., 2018;Fairall et al., 2007;Luhar et al., 2017). In CMAQ, this O_3 deposition to ocean is based on the work of Chang et al. (2004), and uses the oceanic iodine concentration parametrization by MacDonald et al. (2014) (Sarwar et al., 2015). We use the aqueous iodine parameterizations consistent with that in the calculation of inorganic iodine emissions above.

To investigate the contribution from different species and pathways, we in total carried out more than eight simulation runs other than the control run (BASE) in this study. The description of all the simulations and their differences are described in Table 1 (see also Tables S3) and the cross reference between cases and figures in this study is shown in Table S4.

Table 1. Case design in this study.

Simulation case	Species or reactions[a]	Emission rate and ref
BASE	No halogen emissions in the domain	0
BASE_phy	As BASE but excluding[b] reaction N_2O_5(g)+Cl(s), corresponding to SSA_phy below	0
All_high	SSA	High, from Gantt et al. (2015), ≈ Gong (2003) with SST correction from Ovadnevaite et al. (2014)
	I_2 and HOI	High, Carpenter et al. (2013) parameterization and Chance et al. (2014) aqueous iodine
	halocarbons	High, Ordóñez et al. (2012) parameterization and enhancement based on Engel et al. (2019)
All_low	SSA	Low, Gong (2003)
	I_2 and HOI	Low, Carpenter et al. (2013) parameterization and MacDonald et al. (2014) aqueous iodine
	halocarbons	Low, Ordóñez et al. (2012) parameterization and diminution based on Engel et al. (2019)
SSA (SSA_Cl+Br)	Only SSA	As in All_high
SSA_Cl	As SSA but excluding Br	As in All_high
SSA_phy	As SSA_Cl but ~~excluding[†]~~excluding[b] the activation reaction N_2O_5(g)+Cl(s)	As in All_high
SSA_chemCl	SSA_Cl−SSA_phy	--
SSA_chemBr	SSA−SSA_Cl	--
InorgI	Only I_2 and HOI	As in All_high

InorgI_chem	As InorgI but excluding enhanced O_3 dry deposition	Chang et al. (2004) & Sarwar et al. (2015)
O3depo	InorgI−InorgI_chem	--
HaloC	Only halocarbons	As in All_high

~~1~~[a] All cases implement full halogen chemistry as in Sarwar et al. (2019) and Sarwar et al. (2012) except otherwise stated.

[b] The reaction is unchanged but the uptake coefficient of $N_2O_5(g)$ and the yield of $ClNO_2$ are set to 0.

3. Results and discussions

3.1 Performance of the model

To evaluate the performance of our models, O_3, the key species for OH primary production, is compared between simulated and observed data over land (in China~~).~~) and an island (Yonaguni) right east to the Taiwan island. The metrics for evaluation include the average observation (Obs_mean) and simulation (Sim_mean) values, root mean square error (RMSE), normalized mean bias (NMB), normalized mean error (NME), correlation coefficient (*r*), and index of agreement (IOA). The benchmarks are taken from the study of Emery et al. (2017). The statistical metrics of all stations is calculated and the average values are presented in Table 2. We evaluate stations in the three major polluted areas near the seas in mainland China, namely, the North China Plain (NCP), the Yangtze River Delta (YRD), and the Pearl River Delta (PRD) (Fig. S1a). ~~It can be seen that the O_3 concentrations are generally well simulated. Almost of these values meet the benchmarks.~~ For O_3 over the ocean, where is more relevant to this study, we obtain the measurements at the Yonaguni island (24.467°N, 123.011°E) to validate our simulation (data accessible at https://ebas.nilu.no/, last access: January 11, 2022) (Torseth et al., 2012). It can be seen that the O_3 concentrations are also reasonably simulated (Fig. S1b). In addition, adding the halogen emissions (especially with low emission rates) can noticeably lower the bias for the high ozone concentration (i.e., days before July 22) and improve the correlation between observation and simulations, which indicate the potential to improve the capability of ozone forecast at coastal stations by adding the marine-halogen emissions in the regional CTMs. Anyway, except NMB in the YRD, all these values meet the benchmarks (Emery et al., 2017), which shows that the model performance is sufficient for our application.

~~**Table 2. Model performance metrics for 1-hr O_3 in mainland China.**~~

Table 2. Model performance metrics for 1-hr O_3 in mainland China and at Yonaguni island. The benchmarks are taken from Emery et al. (2017).

Region	Obs_mean (μg/m^3)	Sim_mean (μg/m^3)	RMSE (μg/m^3)	NMB	NME	*r*	IOA
NCP	157.84	166.95	47.11	0.06 (< ±0.15)	0.24 (< 0.25)	0.61 (> 0.5)	0.75

YRD	134.46	154.48	52.56	0.15 (< ±0.15)	**0.31** (< 0.25)	0.59 (> 0.5)	0.71
PRD	132.93	141.79	41.48	0. 06 (< ±0.15)	0.23 (< 0.25)	0.74 (> 0.5)	0.83
Whole region	125.13	140.44	38.20	0.13	0.25	0.57	0.70
Yonaguni	39.20	41.82	14.14	0.07 (< ±0.15)	**0.26** (< 0.25)	0.78 (> 0.5)	0.84

Note. There is a threshold value of 40 ppbv for observations in the mainland China as recommended by Emery et al. (2017). For data at Yonaguni no threshold is applied because there is no significant diurnal cycle of O_3 concentration.

Fig. S2 indicate a pretty good performance of the aerosol optical depth (AOD) stimulation that is important for the extinction effect of SSA as discussed in section 3.4.2.

For the relevant halogen species, although the in~~-~~ situ observational data over the marine area ~~is~~ are limited, the model skills of marine halogens could generally be evaluated by the levels of BrO and IO due to their importance in halogen chemistry and the availability of the ship- and aircraft-based data and satellite remote sensing data (Li et al., 2020;Stone et al., 2018;Saiz-Lopez and von Glasow, 2012). Observations of BrO and IO are very rare around the world, especially in East Asia Seas. ~~In a cruise from Japan to Australia,~~ Großmann et al. (2013)~~ measured IO, showing that IO concentration ranges from 1 to 2.2 pptv, with a typical daytime value ~1 pptv.~~ The available measurements of mean concentrations of BrO in Western Pacific show 1.0, 1.7 and <0.5 pptv in three flights Koenig et al. (2017) and 0.69 pptv (Le Breton et al., 2017) during two related campaigns (CONTRAST and CAST). These values are generally smaller than measurements in the Atlantic Ocean (e.g., Read et al., 2008). In addition, according to the global model results (Zhu et al., 2019) and satellite remote sensing (e.g., http://www.doas-bremen.de/bro_from_gome.htm, last access: 4 June 2021), surface BrO concentrations have large annual variations in the Western Pacific, with the largest values in January ~~while~~ and the smallest values in July. In a cruise in October from Japan to Australia, Großmann et al. (2013) measured IO, showing that the daytime average of the IO concentration ranges from ~0.5 to ~1.5 pptv, with a typical daytime value ~1 pptv. Previous model results showed that surface IO in the Western Pacific has a significant seasonal variation, peaks in summer (Huang et al., 2020) and the difference between July and October is about 0.2–0.4 pptv according to their Figs. 3m,p. Therefore, it is expected that our simulation values (in July) will be slightly larger than the values reported by Großmann et al. (2013). Moreover, since modelled IO also decreases with height in the lower troposphere (see Fig. 2 of Huang et al. (2020)), the surface IO is also expected to be slightly larger than the boundary-layer average of IO.

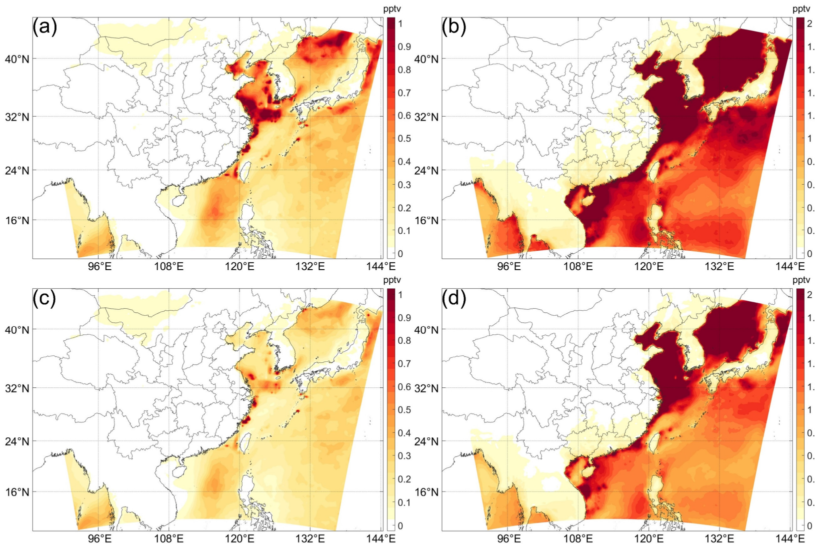

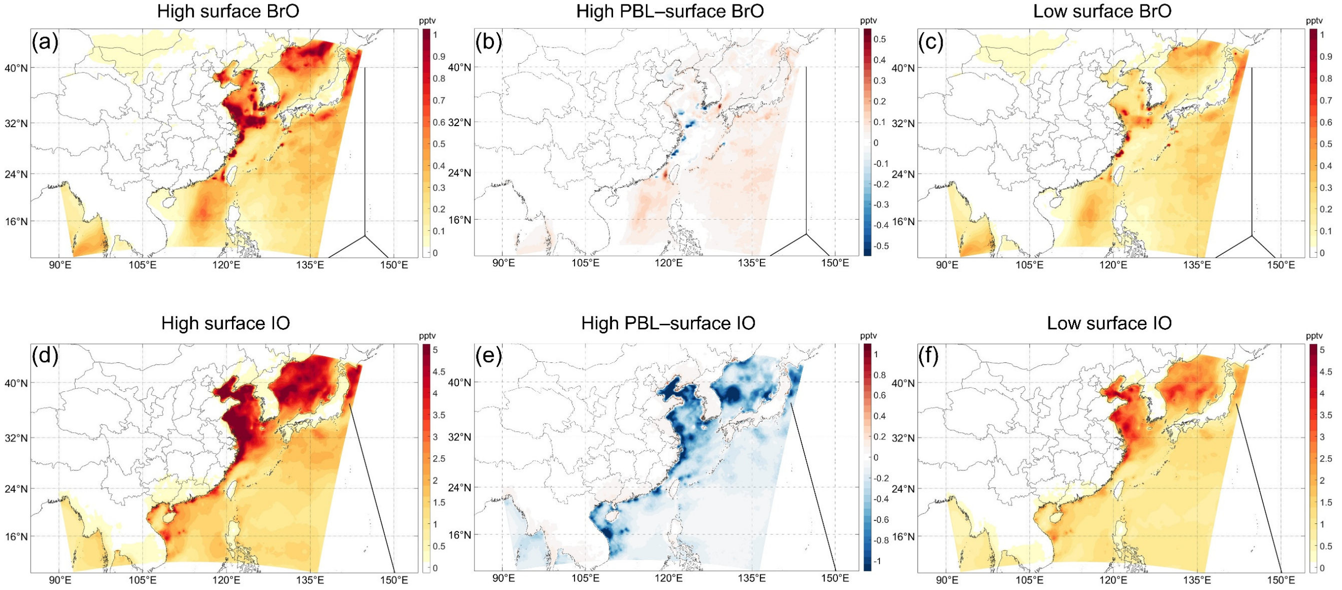

Figure 1. Daytime (local time 8:00–16:00) average of (a) ~~BrO~~surface BrO, (b) difference between planetary boundary layer (PBL) and ~~(b) IO~~surface BrO, for high emission rate~~. (c)~~, and (~~d) are~~ c) surface BrO for low emission rate. (d)–(f) are for IO. The black lines indicate roughly the trajectories of flights or cruise in previous studies reporting relevant measurements (see Table 3).

Table 3. Comparison of BrO and IO in the Philippine Sea in our simulations (surface layer) with observations and simulations reported in other studies.

Mean/max	Platform

	Simulation, low emission rate	Simulation, high emission rate	Observation or model		
BrO (pptv)	0.2/0.9 Jul	0.25/1.2 Jul	~1/2.9^{a,1} Jan & Feb		Flights around Guam (line in Figs. 1a–c) < ~500m
			0.69/1.71^{2} Jan		
			~1/>2^{3} Jan	~0.3/>0.6^{3} Jul	GEOS-Chem surface layer
IO (pptv)	1.0/1.8 Jul	1.4/2.5 Jul	~1~~/2.2^{4}~~/~1.5^{4} Oct		Cruise from Japan to Australia (line in Figs. 1d–f) PBL
			Average Jul > Oct by ~0.2–0.4^{5}		CMAQ surface layer

^{a} only data at altitudes below 500 m.

^{1} Koenig et al. (2017), ^{2} Le Breton et al. (2017), ^{3} Zhu et al. (2019)~~, ^{4}~~ Großmann et al. (2013)~~.~~, ^{4} Großmann et al. (2013), ^{5} Huang et al. (2020).

Figure 1 shows the daytime (local time 8:00-16:00) average BrO and IO simulated in our studies. Due to the lack of observation data in the coastal seas for comparison, we only discuss the results in the Philippine Sea (i.e., the open ocean east to the line connecting the Philippines, Taiwan, and Japan). In this sea, the concentrations of BrO and IO are generally lower than nearshore areas. The maximum mean values of the daytime BrO and IO are 1.2 (0.9) and 2.5 (1.8) for high (low) emissions; for the average over all these grids, the daytime BrO is about 0.25 (0.2) pptv, while IO about 1.4 (1.0) pptv for high (low) emission rates. For boundary-layer average, the values for IO are lower than surface values by ~0.08 pptv for grid average and by ~0.4 pptv for grid maximum in the Philippine Sea in All_high case (Fig. 1d) (due to the storage limitation, we did not output upper-layer results in All_low case). Different from IO, BrO does not decrease with height in the lower ~500m in the study of Huang et al. (2020), and our simulations also show that boundary-layer average of BrO is slightly larger than surface values by ~0.05 pptv (Fig. 1b).

Table 3 lists the comparison of the available measurements and global model results in the area and our model results. It can be seen that our model results generally agree well with measurements and other model results. It should be emphasized that the comparison is only indirect and there is a lack of data for even indirect comparison in the nearshore areas where the IO concentration is the largest. Since the inorganic iodine emission is closely related to O_3 concentration which is high in the nearshore areas due to the outflow from the continent, the higher concentration of IO is reasonable, and in other regions, observations also support a very high concentration of IO in nearshore areas (Saiz-Lopez and von Glasow, 2012), but nevertheless, relevant observations are expected for a better validation.

3.2 The changes of OH production rate (P_{OH}) and concentration

Figure 2 illustrates the halogen-induced changes of P_{OH} and OH concentration in All_high (all halogen species high emission rates) and All_low (all halogen species low emission rates) cases. ΔP_{OH} and ΔOH with both high and low emission rates all have similar spatial distributions but with different magnitudes. The most significant changes of P_{OH} and OH appear in the marine atmosphere (Fig. 2). The impacts are very complicated, with negative ΔP_{OH} and ΔOH in the middle area of the ocean while positive in the north and south parts of the ocean in the domain, but the area with negative impacts is larger than that with positive impacts. The decreases of OH can reach ~13% and ~8% (ΔP_{OH} ~15% and ~10%) in the Philippine Sea and the increase can reach ~11% and ~9% (ΔP_{OH} ~9% and ~7%) in the Bohai Sea, with high and low emission rate, respectively. This is in line with previous studies that generally showed decrease of globally-averaged OH but certain increase in some regions due to halogen chemistry (e.g., Sherwen et al., 2016;Stone et al., 2018). More specifically, in the East Asia seas, the studies of Stone et al. (2018), Wang et al. (2019) and Sherwen et al. (2016) generally showed a slight decrease (<~5%) of annual-averaged surface OH while Stone et al. (2018) also showed a slight increase in some regions. For studies in July, the study of Li et al. (2019) showed a decrease of monthly averaged surface OH in the Atlantic Ocean near to Europe but an increase in the Mediterranean Sea and the Baltic Sea. The decrease in the Atlantic Ocean can reach ~20% in the middle latitude. In the Indian Ocean, Mahajan et al. (2021) showed a slight decrease (<5%) of monthly averaged surface OH near the Indian subcontinent while ~~increase~~ increasing (<10%) near the equator, and the area with decreased OH is larger than that with increased OH in their model domain.

In the coastal areas the absolute changes of P_{OH} and OH can be comparable to or even larger than that over the ocean, but the relative values are relatively small due to the large absolute value over land (Figs. 2b, d, f, h). In the Greater Bay Area the decreases of monthly P_{OH} and OH are the largest, which can reach ~3–5% and ~4–6%, respectively (Figs. 2b,f).

Generally speaking, our results are comparable to previous studies, showing overall negative halogen-induced ΔOH but with complicated spatial distribution of negative and positive ΔOH (and ΔP_{OH}), especially in nearshore area. Previous studies have qualitatively and partially explained the reasons why halogens have such a complicated impact on OH, as the two pathways by which halogens influence OH (i.e., enhanced HO_2 conversion by XO and O_3 consumption by X atoms) have opposite impacts on OH (e.g., Stone et al., 2018). However, the complicated spatial distribution of negative and positive ΔOH indicates a complicated interaction of the pathways. Furthermore, it is unclear whether there are other important pathways by which halogens influence OH. Therefore, in order to better understand the impacts of halogens on OH, and more specifically, to understand why halogens increase OH in certain regions (especially nearshore area) but decrease in other regions, we need to find out all possible important pathways, and to further analyze the controlling factors of the strengths of the pathways.

In the following, we will further analyze the causes of such a complicated distribution. Since the spatial distributions of relative ΔP_{OH} and ΔOH are very similar despite the small difference in magnitudes, and the OH chemistry is generally discussed in terms of P_{OH} in the literature (e.g., Tan et al., 2019;Hofzumahaus et al., 2009;Whalley et al., 2021) and we can directly separate different pathways by which influence P_{OH}, we will focus on P_{OH} in the following. Besides, because the patterns of ΔP_{OH} and ΔOH (Fig. 2), as well as the IRR results (Figs. 4 and ~~S2~~S3), are quite similar in the All_high and All_low cases (Fig. 2), we will mainly focus on cases with high emission rates.

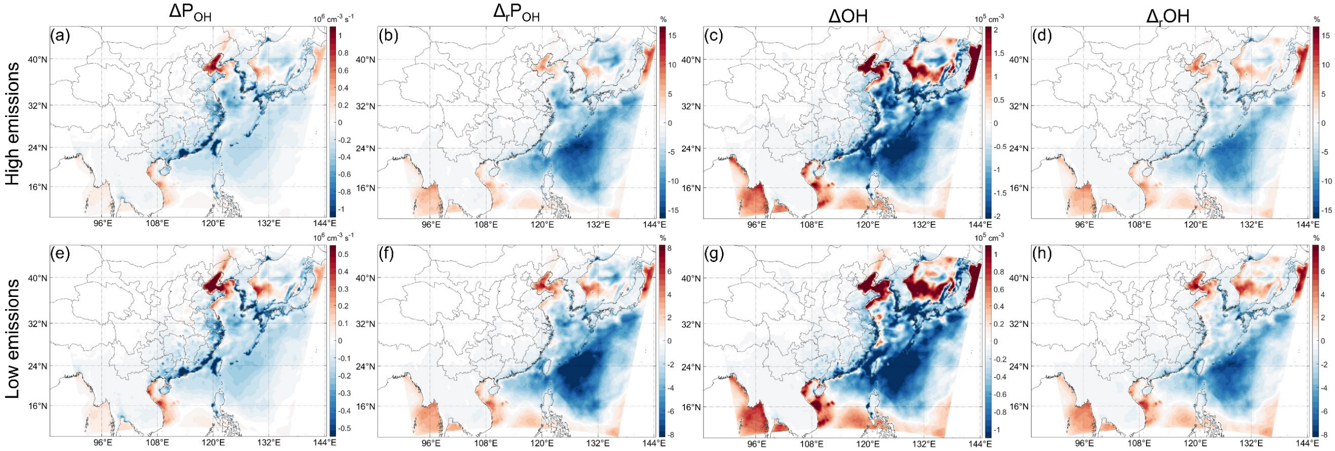

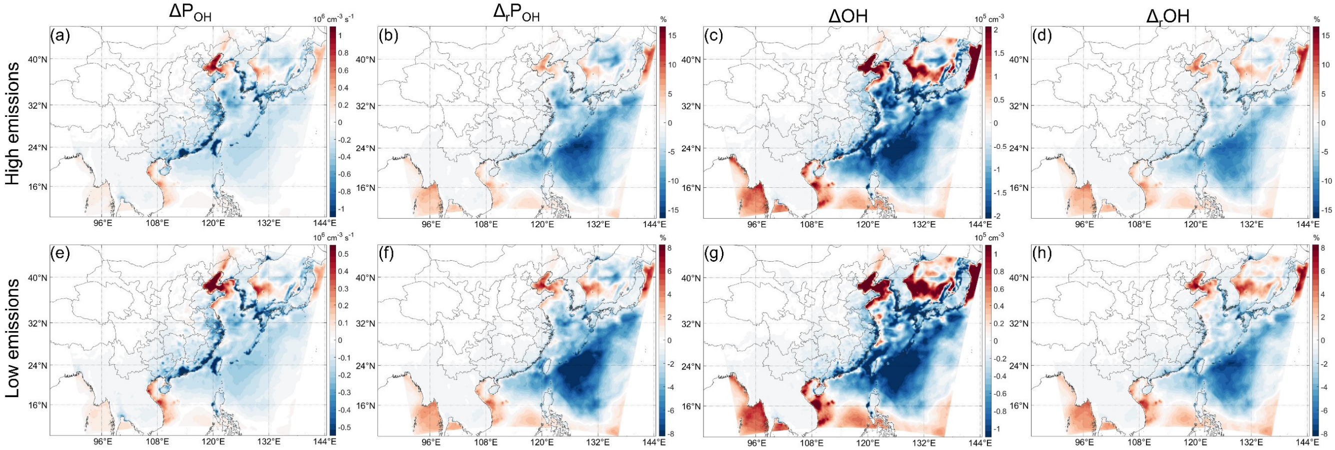

Figure 2. Change or relative change compared to BASE case of monthly averaged surface-layer P_{OH} and OH in All_high case (first row) and All_low case (second row). The subscript "r" denotes "relative". Note the different scales in the All_high and All_low cases, the latter exactly a half to the former.

3.3 Quantification of different pathways' contributions

As mentioned above, there is complexity in the cause of the ΔP_{OH}. In this section, IRR is used to unravel important chemical reactions in changing P_{OH}. The main sources of OH in the CB6 mechanism of CMAQ model include primary sources and secondary sources. Primary sources include the photolysis of O_3~~,~~ (through the reaction $O(^1D)+H_2O$, which will not always be explicitly stated in the following), HONO, and H_2O_2, and ozonolysis of some alkenes. The secondary source is mainly the reactions HO_2+Y (Y=NO, O_3, etc.). With halogen chemistry, an additional ~~primary~~ source, HOX photolysis, needs to be considered~~.~~ as HOI can be directly emitted and can be very rapidly cycled. The changes of P_{OH} due to the change of all these sources (denoted as ΔP_{OH_XX} in the following where XX is clear from the context) based on IRR analysis are ~~illustrated in Fig. 3. It can be seen that~~ quantified. According to the IRR results, we only focus on the main three changes ~~of~~ (photolysis of O_3 and HOX, and the reaction HO_2+Y ~~are the main contributors to ΔP_{OH}. The photolysis of H_2O_2~~) (Fig. 3a–c). -Since the changes ~~small, while the~~ of other ~~two~~ sources ~~almost remain unchanged. Other minor sources, including OH from RO_2, OH from FORM+O, as well as the photolysis of a hydroperoxyaldehyde from isoprene-derived RO_2 isomerization, contribute negligibly to ΔP_{OH}~~are ignorable (Fig. 3d), we do not show it by individual. We denote the halogen-induced change of these sources as pathways by which halogens influence OH and therefore there are three main pathways through which marine-emitted halogens influence P_{OH}, i.e., P_{OH_O1D}, P_{OH_HO2}, and P_{OH_HOX}.

In line with previous studies, the results show the change of O_3 and the addition of HOX are the two most important pathways by which halogens influence P_{OH} (Stone et al., 2018). ΔP_{OH} caused by the change of O_3 and HOX photolysis (denoted as ΔP_{OH_O1D} and ΔP_{OH_HOX} respectively) are very large in the north part of the ocean in the domain, especially in the Bohai sea and the Yellow sea, which is probably a result of the higher concentration of related species such as O_3 that is commonly reported at high concentration in the midlatitude in summer (e.g., Gao et al., 2020b;Lu et al., 2019b;Hu et al., 2017). ΔP_{OH_HOX} (Fig. 3f) can reach 4×10^6 cm^{-3} s^{-1} (~0.6 ppbv h^{-1}) for the whole-day average and 1×10^7 cm^{-3} s^{-1} (~1.5 ppbv h^{-1}) for the daytime average. Our results show that ~~Since~~ HOX is ~~a primary~~an important source of OH~~,~~ (may be compared to urban-area HONO) over the ocean, and but it was generally ignored in the previous HO*x* budget studies ~~generally ignoreddid not consider it~~ (e.g., Tan et al., 2019;Hofzumahaus et al., 2009;Whalley et al., 2021). Therefore, our results indicate ~~the large production rate of OH from HOX suggests~~there is the necessity to measure HOX in HO*x* budget studies under the potential influence of marine atmosphere.

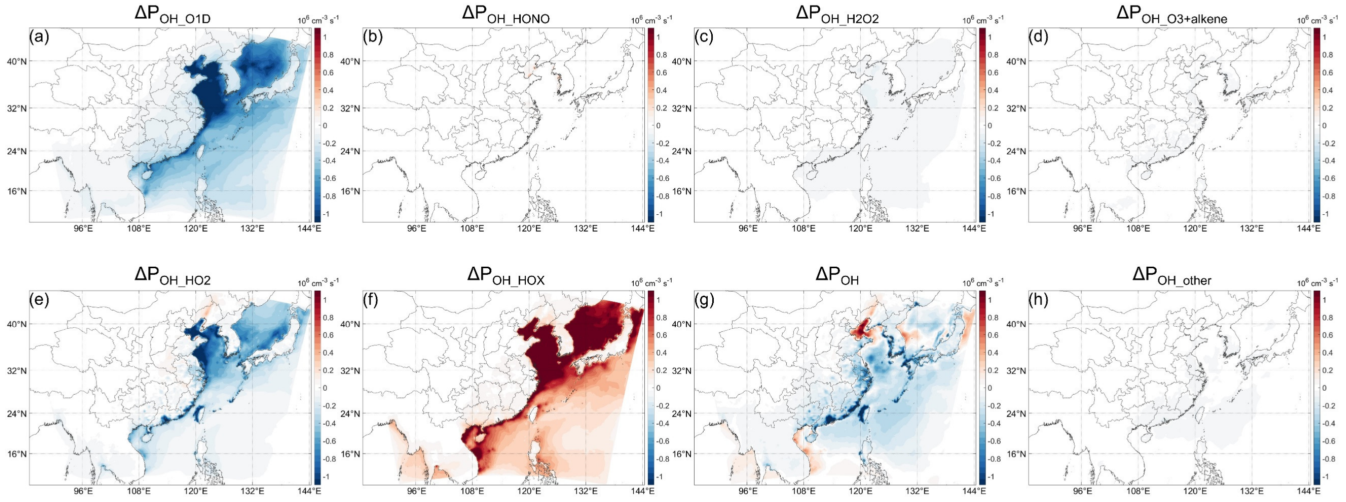

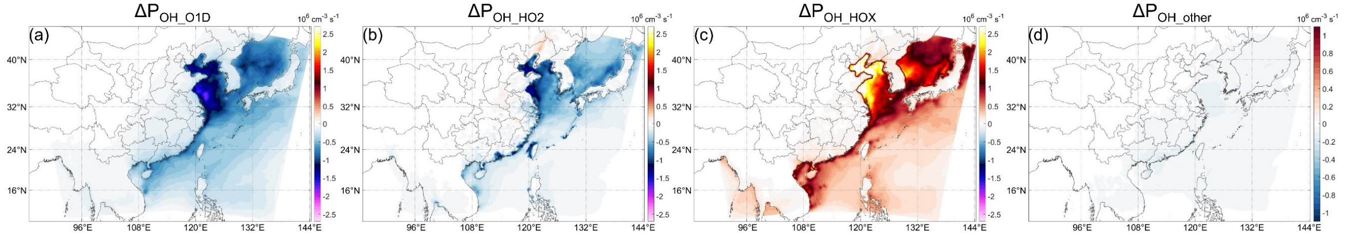

Figure 3. ~~Change~~Decomposition of Fig. 2a for different pathways: change of P_{OH} (All_high–BASE case) caused by the changes of (a) O(^{1}D) (ΔP_{OH_O1D}), (b) ~~HONO+hv (ΔP_{OH_HONO}), (c) H_2O_2+hv (ΔP_{OH_H2O2}), (d) O_3+alkene ($\Delta P_{OH\_O3+alkene}$), (e)~~ HO_2+Y (ΔP_{OH_HO2}, Y=NO, O_3, etc.~~)~~.), and (~~f~~c) HOX+hv (ΔP_{OH_HOX}~~). (g) is the net ΔP_{OH}, the same as Fig. 2a. (h) is the difference between ΔP_{OH}~~), and ~~the~~(d) other pathways (=Fig. 2a minus sum of (a)–(~~f).~~c)). The red and blue color scales are the same in (a)–(d).

In addition to ΔP_{OH_O1D} and ΔP_{OH_HOX}, ΔP_{OH_HO2} is also very important to ΔP_{OH} as shown in Fig. 3~~e~~b~~. But, ΔP_{OH_HO2} was generally ignored in previous CTM studies, and box model studies cannot accurately model the impact of the change of HO_2+Y on OH because NO and O_3 are observation-constrained (Stone et al., 2018;Whalley et al., 2010). The contribution of this pathway to the change of P_{OH} is significant~~. If we considered only ΔP_{OH_O1D} and ΔP_{OH_HOX}, only a relatively small area close to the Taiwan island would show negative ΔP_{OH} and the general impacts of halogens on OH would be positive (compare Figs. ~~3g~~2a and ~~S3~~S4a).

As mentioned above, the production rate of OH from HOX is very large. However, this large production rate is canceled by the large decrease of ΔP_{OH_O1D} and ΔP_{OH_HO2} (Figs. 3a,e), resulting the relatively small net ΔP_{OH} compared to ΔP_{OH_O1D} and ΔP_{OH_HOX} (and even ΔP_{OH_HO2} for many regions) over the ocean but still significant along the coastal areas (Fig. 3). It can be seen that the cancel-out effect of the three pathways with different signs result in the complicated spatial distribution of ΔP_{OH}, making ΔP_{OH} positive in the areas with larger ΔP_{OH_HOX} and negative otherwise. From these three pathways themselves, however, it is difficult to explain under what conditions ΔP_{OH_HOX} will be stronger than the other two pathways, and therefore difficult to explain why ΔP_{OH} is generally positive in the nearshore areas while negative in the open ocean. Then we need to further analyze the details of the processes influencing the strengths of these three pathways.

3.4 Factors influencing the strengths of the three pathways

3.4.1 Overview of the contributions from different marine-emitted species

There are several factors that can change the strengths of the three main sources of OH (Fig. S5~~4~~). Some of these factors are independent, some are interrelated. The independent factors include decrease of O_3 photolysis rate ($J(O^1D)$) and O_3 concentration by SSA-induced light extinction, and enhancement of O_3 deposition by oceanic iodine. The interrelated factors are generally closely related to halogen chemistry of which the most important reactions are the below three that for all three halogen elements and the fourth for Cl only (Saiz-Lopez and von Glasow, 2012;Simpson et al., 2015):

$$X + O_3 \rightarrow XO + O_2 \qquad (R1)$$

$$XO + HO_2 \rightarrow HOX + O_2 \qquad (R2)$$

$$HOX + h\nu \rightarrow X + OH \qquad (R3)$$

$$Cl + VOCs \xrightarrow{O_2} RO_2 + HCl \qquad (R4)$$

For convenience, we also list the two reactions producing OH that are relevant to R1–R3 and have been mentioned above:

$$O_3 + h\nu \rightarrow O^1D + O_2 \qquad (R5a)$$

$$O(^1D) + H_2O \rightarrow 2OH \qquad (R5b)$$

$$HO_2 + NO \rightarrow OH + NO_2 \qquad (R6a)$$

$$HO_2 + O_3 \rightarrow OH + 2O_2 \qquad (R6b)$$

Since these factors are generally species-related, we separately modeled the impacts of different halogen species in addition to the case with all emissions (All_high) (Table 1). The results are shown in Fig. 4. It can be seen that the most significant contributors to the three pathways are inorganic iodine (Fig. 4e–g). However, the three pathways cancel out each other to a large extent and the resultant ΔP_{OH} is relatively small. Nevertheless, the impact of inorganic iodine is more ~~positive~~pronounced than that of the all species together~~.~~ (Figs. 2a and 4e). The contribution of SSA to ΔP_{OH} is notable, comparable to that of inorganic iodine in most regions. There is positive contribution of SSA to ΔP_{OH} in the Bohai Sea and surroundings, while in other regions the contribution is negative. The negative contribution again neutralizes the positive contribution of inorganic iodine, resulting in ~~a smaller~~the more negative ΔP_{OH} in All_high case (Fig. ~~3g~~2a) than in InorgI case (Fig. 4e). The contribution of halocarbons is relatively small and restricted to a small area near to the China coastline. Besides, the interactions between these three types of emitted species (Fig.4m) have very similar impacts with halocarbons (Fig. 4i) but with opposing sign. Since we only focus on major contributions of different halogen species to ΔP_{OH}, we will not go into the details about the rest interactions of the three types of halogen emissions, and therefore we also do not discuss the influences of halocarbons in the following as they roughly cancel out the effects of the interactions. It should be noted, however, this does not imply that the interactions are caused by halocarbons.

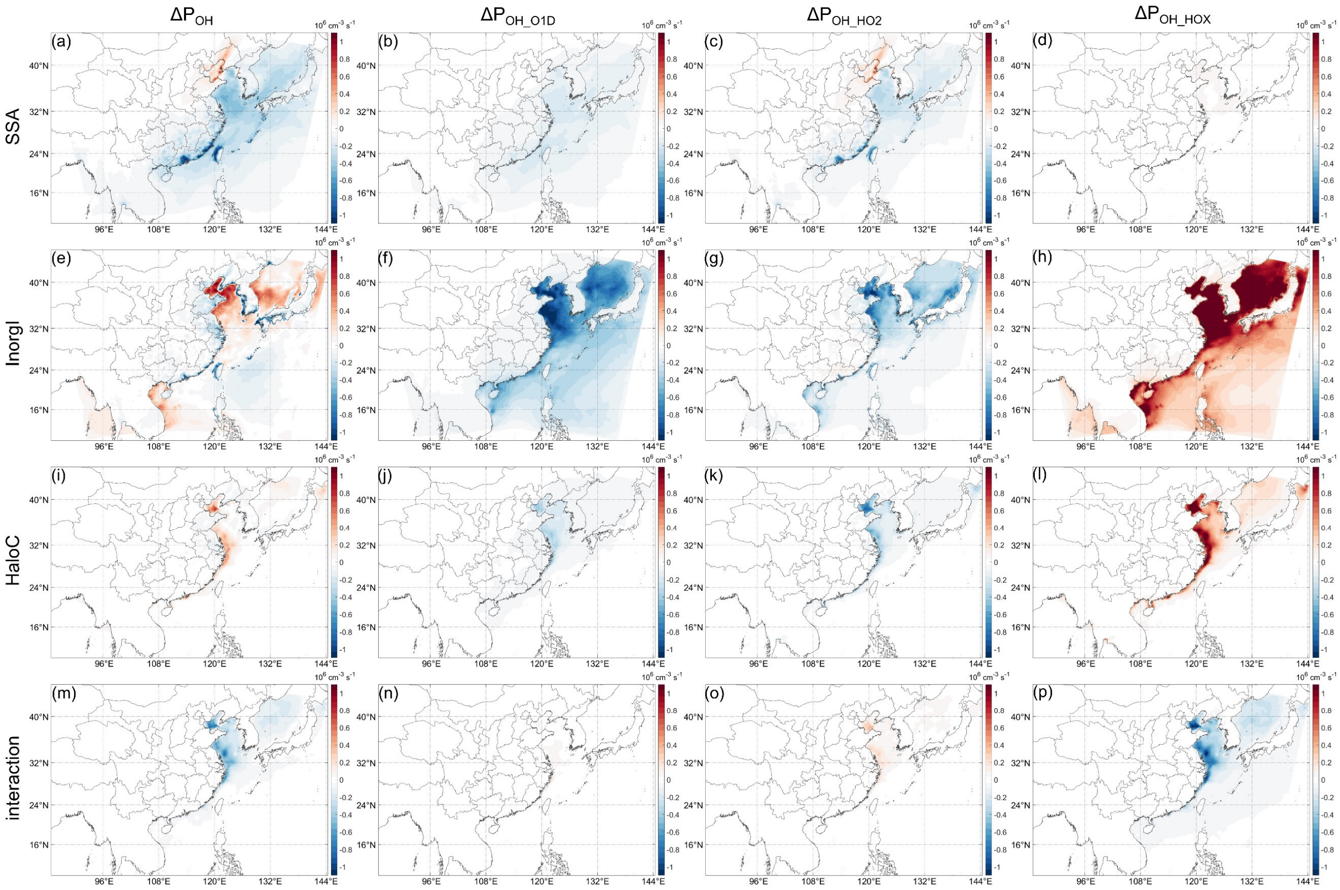
ΔP_OH
ΔP_OH_O1D
ΔP_OH_HO2
ΔP_OH_HOX
SSA
InorgI
HaloC
interaction
(a)
(b)
(c)
(d)
(e)
(f)
(g)
(h)
(i)
(j)
(k)
(l)
(m)
(n)
(o)
(p)
10^6 cm^-3 s^-1
1
0.8
0.6
0.4
0.2
0
-0.2
-0.4
-0.6
-0.8
-1
40°N
32°N
24°N
16°N
96°E
108°E
120°E
132°E
144°E

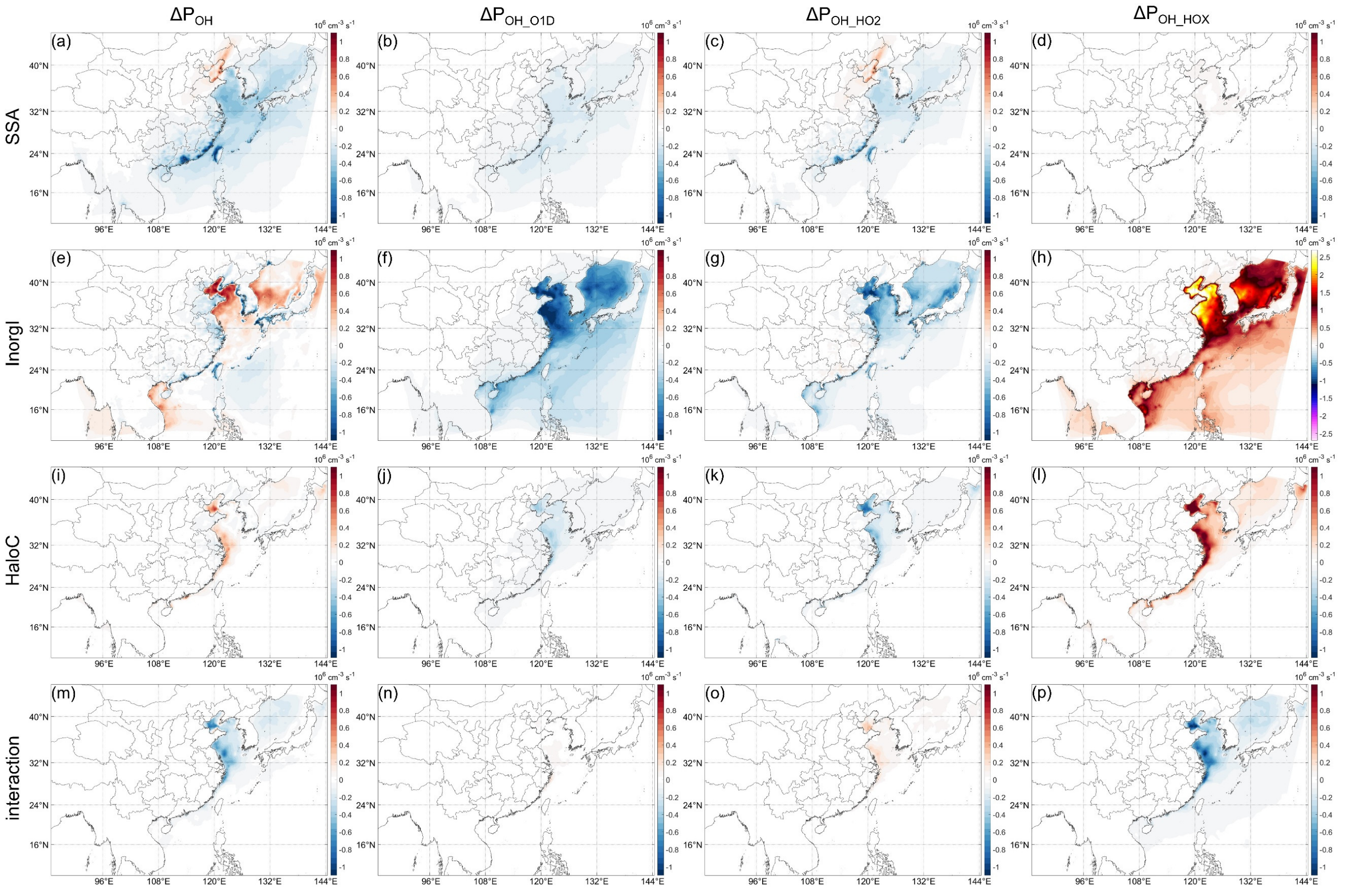

Figure 4. ~~The changes~~Decomposition of ~~net OH production rate (ΔP_{OH}) and that induced by~~Fig. 3 for different ~~pathways (ΔP_{OH_O1D}, ΔP_{OH_HO2}, and ΔP_{OH_HOX}) compared to BASE case~~halogen species. (a)–(d), (e)–(h), and (i)–(l) are results for SSA, InorgI, and HaloC case, respectively. (m)–(p) are the residue between All_high and SSA+InorgI+HaloC, representing the interactions of different halogen species. The red and blue color scales are the same in (a)–(p).

3.4.2 Physical and chemical contributions of SSA emission

Regarding SSA, whose components are mainly Cl^- ions and inert non-volatile cations (NVCs, including Na~~,~~$^+$, K~~, Ca,~~$^+$, Ca^{2+}, and ~~Mg),~~Mg^{2+}), with minor contribution from sulfate and Br^- ions, these emissions (see Fig. S6c,d for the emission rates) could influence OH through both actinic flux and chemical effects of Cl and Br~~ (Fig. ~~. The SSA impact on OH (Fig. 4a–d SSA) is further decomposed into the impact of the extinction effect of SSA, Cl chemistry, and Br chemistry (Fig. 5). Figure 5 indicates that the most important factor that determines the negative impact of SSA on P_{OH} (Fig. 4a) is its extinction effect (Fig. 5a–d). The decrease of actinic flux caused by the extinction effect of SSA can decrease the photolysis rate constant of O_3 ($J(O^1D)$) and the O_3 concentration ~~at the same time (Fig. S5), while the Cl and Br chemistry can increase or decrease O_3 and HOx radicals.~~(probably through influencing $J(NO_2)$, see e.g., Gao et al. (2020a)) at the same time (Fig. S6a,b), which will in turn decrease the OH production from O_3 photolysis (R5). ~~Figure 5 indicates that the most important factor that~~

~~determines the negative impact of SSA on P_{OH} (Fig. 4a) is its extinction effect.~~ The negative impacts of Br chemistry are very small compared to this extinction effect. Besides the overall large impacts, the importance of the SSA extinction effect is also embodied in its impact on the continental atmosphere. As shown in Figs 4a,e,i the ΔP_{OH} over land induced by SSA is the most significant among the three halogen emissions, and here we know that the relatively large decrease of P_{OH} in southern China is caused by the extinction effect of SSA. In the Greater Bay Area the decrease of monthly P_{OH} caused by SSA can reach ~3% (~~with~~Fig. 6a) (hourly $\Delta_r P_{OH}$ up to 30% in the daytime~~ maximum close to 30%).~~). Therefore, even without halogen chemistry, adding SSA emissions in CTM studies may be important for atmospheric chemistry.

Another important factor that influences P_{OH} is the Cl chemistry (~~Fig~~Figs. 5e−h and 6b). Similar to previous studies, Cl chemistry has positive impacts on ΔP_{OH} because Cl can oxidize VOCs, which can both come from anthropogenic and oceanic source (Yu and Li, 2021), efficiently and produce RO_2 radicals (R4) as shown in Fig. 5e (Li et al., 2020;Wang et al., 2020;Simpson et al., 2015). ~~Indeed~~As such, the change of P_{OH} by Cl chemistry (Fig. 5e) is mostly through the change of OH production from HO_2 (Fig. ~~5f~~5g). The impacts of Cl chemistry are most significant in the Bohai Sea and surroundings. ~~In~~As shown in Fig. S7, in these areas, the concentration of $ClNO_2$ (the key species for the activation of SSA Cl) are higher than other regions (Fig. S7a) and the Cl reactivity (k_{Cl}, $=\sum k_{Cl+VOC}\times[VOC]$) ~~are higher than other regions (Fig. S6),~~is very high, resulting in the larger impact of the Cl chemistry. $ClNO_2$ is a product of N_2O_5 with particulate Cl, and N_2O_5 is a product of NO_2 and NO_3 radical (e.g., Yu et al., 2020). Therefore, the larger impacts of Cl chemistry in the Bohai Sea and surroundings probably reflect the influence of higher NOx ~~and VOCs~~ in the areas. The impact of Br chemistry on P_{OH} is quite small ~~because it can merely influence O_3 concentration~~in general (Figs. 5i–l), and we will not discuss it further~~.~~ (see more discussion about Br chemistry in section 3.5). Nevertheless, the results from Br chemistry emphasize the importance of pathway P_{OH_HO2} in interpreting the roles of halogens in influencing HOx cycling: When considering the influence of halogens on HOx, it is believed that XO will shift the HOx balance to OH in general (e.g., Li et al., 2020;Stone et al., 2018;Saiz-Lopez and von Glasow, 2012). But these results are derived without consider the indirect influence of halogens on R6 (i.e., pathway 2, P_{OH_HO2}, in our study). In our study, when the inhibition of halogen chemistry on the HO_2 conversion to OH through HO_2+Y is considered (R6), only IO can uniformly enhance the HO_2 conversion and BrO cannot in some areas (compare Figs. 5k and 5l, or see Fig. S4b) which is probably because the lower reactivity of BrO with HO_2 (see also discussion in section 3.4.2 of Whalley et al. (2010)).

In regards to the three main pathways discussed in section 3.3, the physical contribution of SSA is achieved not only through the decrease of the photolysis of O_3 (~~both~~ $J(O^1D)$ and the O_3 concentration) (Fig. 5b), but also through the decrease of HO_2 conversion to OH (Fig. 5c) which is probably feedback induced by the decrease of O_3 photolysis because HO_2 production is little influenced by photolysis change. In contrast, the chemical contribution of SSA Cl is achieved through the increase of RO_2~~,~~ that can rapidly react with NO to form HO_2 (Seinfeld and Pandis, 2016), and therefore the second pathway, OH from HO_2, is more prominent (Fig. 5g), while the increase of O_3 concentration is of minor importance (Fig. 5f).

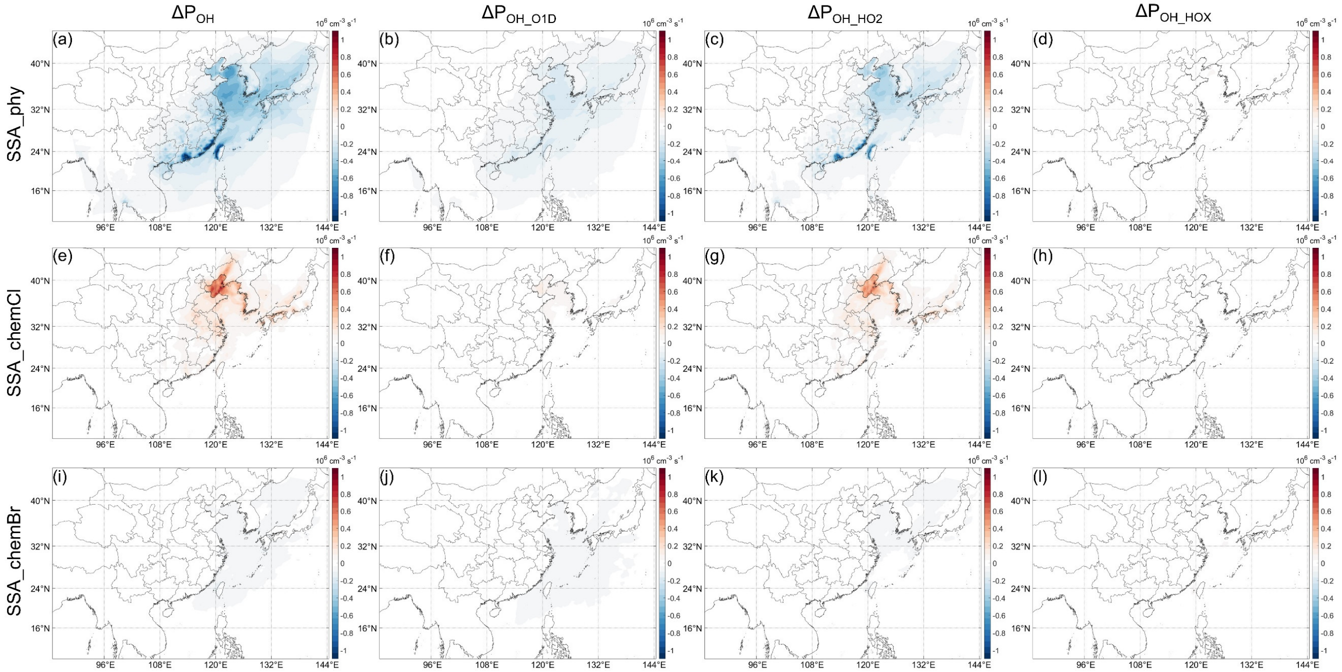

Fig. 5. **~~The~~Decomposition of Fig. 4a–d (SSA): the changes of ~~net OH production rate (ΔP_{OH}) and that induced by different pathways (Δ~~P_{OH} , P_{OH_O1D}, ΔP_{OH_HO2}, and ΔP_{OH_HOX}~~) compared to BASE case,~~ caused by (a)–(d) the extinction effect of SSA, denoted as SSA_phy, (e)–(h) Cl chemistry (only the activation of Cl through $ClNO_2$), and (i)–(l) Br chemistry.**

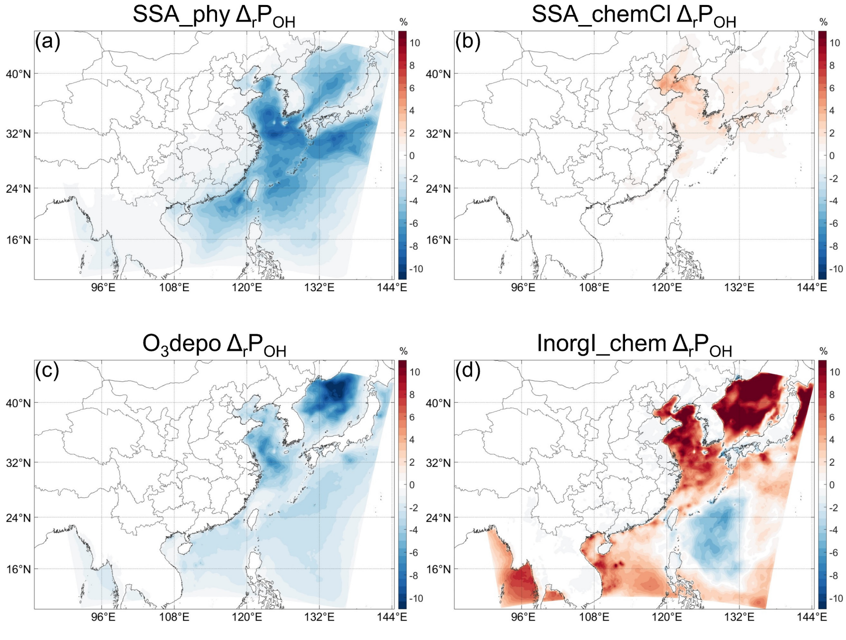

Figure 6. Relative change of P_{OH} compared to BASE, caused by (a) SSA extinction effect, (b) SSA Cl chemistry, (c) enhanced O_3 deposition by aqueous iodine and (d) atmospheric inorganic iodine chemistry.

3.4.3 Physical and chemical contributions of inorganic iodine species, and the interactions between O_3 and iodine chemistry

~~Regarding the contributions from inorganic iodine species on ΔP_{OH}, the effects from the enhanced O_3 deposition by iodine ion in the ocean~~Regarding the contributions from inorganic iodine species on ΔP_{OH}, the indirect effects from the enhanced O_3 deposition by iodine ion in the ocean (e.g., Pound et al., 2020) and atmospheric iodine chemistry (including the direct emission of HOI) should be considered. The change of P_{OH} caused by the enhanced O_3 deposition is shown in Fig. 7a. ~~The~~This O_3-deposition-induced decrease of P_{OH} is most significant in the Bohai and Yellow Sea, where it can reach ~0.4×10^6 cm^{-3} s^{-1}, corresponding to ~6% (~~daytime~~ hourly ~~maximum >~~ $\Delta_r P_{OH}$ can reach >30% in the daytime) in the Yellow Sea relative to P_{OH} in the BASE case (Fig. 6c). The larger absolute decrease of P_{OH} (Fig. 7a) is probably caused by the higher deposition of O_3 in the Bohai and Yellow Sea because of the higher O_3 concentration there as mentioned above~~.~~ (see also Fig. 8). For the relative change, the decrease of P_{OH} is most significant in the Sea of Japan, where the relative decrease can reach more than 10% (~~daytime~~ hourly ~~maximum >~~ $\Delta_r P_{OH}$ can reach >45% in the daytime) (Fig. 6c). ~~More specifically, this~~ By decomposing to different pathways, the decrease of P_{OH} induced by O_3 deposition are caused by the decrease of O_3 (P_{OH_O1D}, Fig. 7b), and by the decrease of HOX photolysis (P_{OH_HOX}, Fig. 7d) which probably results from the slower cycling of HOI through reactions R1–R3 due to the lower O_3 concentration.

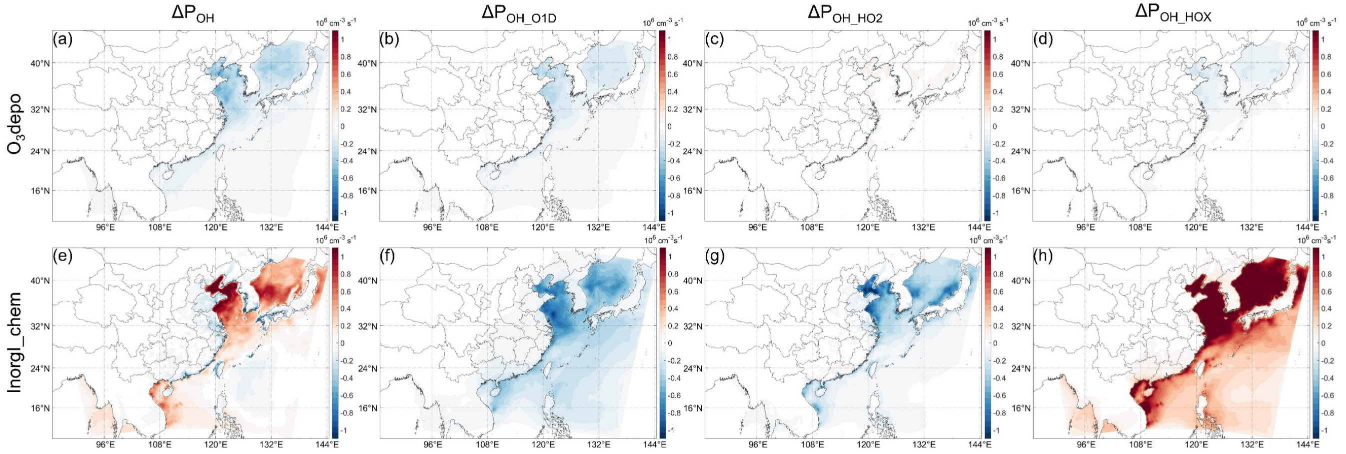

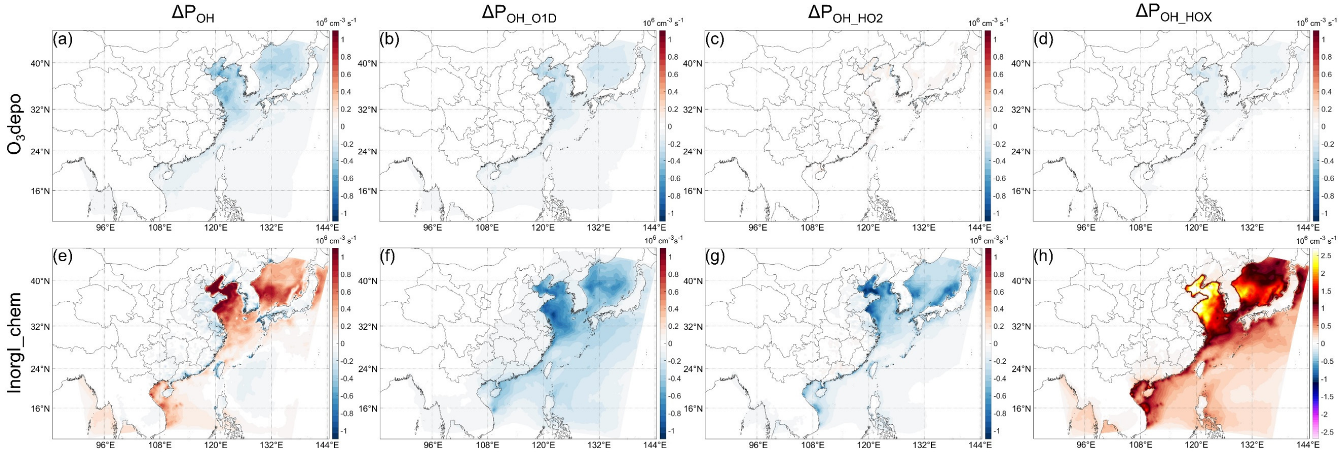

Figure 7. ~~The~~Decomposition of Fig. 4e–h (InorgI): the changes of net OH production rate ~~(ΔP_{OH}) and that induced by different pathways (ΔP_{OH_O1D}, ΔP_{OH_HO2}, and ΔP_{OH_HOX}) compared to BASE case,~~ caused by (a)–(~~h~~d) the enhanced O_3 deposition by oceanic iodine ions and (e)–(h) atmospheric iodine chemistry (including direct HOI emission). The red and blue color scales are the same in (a)–(h).

Regarding the contributions from the atmospheric iodine chemistry on ΔP_{OH}, it has general positive impact on P_{OH} except in a limited ~~areas~~area (Figs. 6d and 7e). More specifically, the decrease of ΔP_{OH} is relatively significant in the Philippine Sea (~~Figs. 6d, 7e). The direct emission of HOI has only very small contribution (Fig. S7) and we will not discuss it further.~~up to ~8% of BASE case). The positive ΔP_{OH} in the Bohai and Yellow Sea can reach more than ~~1×10^{6} cm^{-3} s^{-1} ($\sim$~~10% of BASE case~~) (Fig. 6d). In the Sea of Japan,~~, and the relative increase can reach more than 15~~%.~~% in the Sea of Japan. The changes of P_{OH} caused by the atmospheric iodine chemistry from different pathway are shown in Fig. 7e–h. It can be seen in Fig. 7 that the contributions of three pathways are all significantly influenced by iodine chemistry. Different from Cl chemistry, iodine chemistry can both increase P_{OH} via R3 (Fig. 7h) and decrease P_{OH} via R1–R2 (Figs. 7f–g). ~~It is obvious that the competition between reactions R1/R2 and R3 can influence the net effect (positive or negative) of the iodine-chemistry-induced ΔP_{OH}. However, further analysis shows that the negative iodine-chemistry-induced ΔP_{OH} in the Philippine Sea is unlikely caused by the competition between O_3 loss rate and HOI cycling rate because these two rates are similar in the whole domain (Fig. S8c), but probably by the non-uniform response of O_3 concentration to the O_3 loss rate (Fig. S8e): O_3 concentration decreases more in the Philippine Sea than that is consumed by iodine there locally (see more details in SI). Compared to the physical net contribution of the inorganic iodine species, the net contribution of the iodine chemistry dominates the ΔP_{OH} pattern related to iodine shown in Fig. 4e.~~

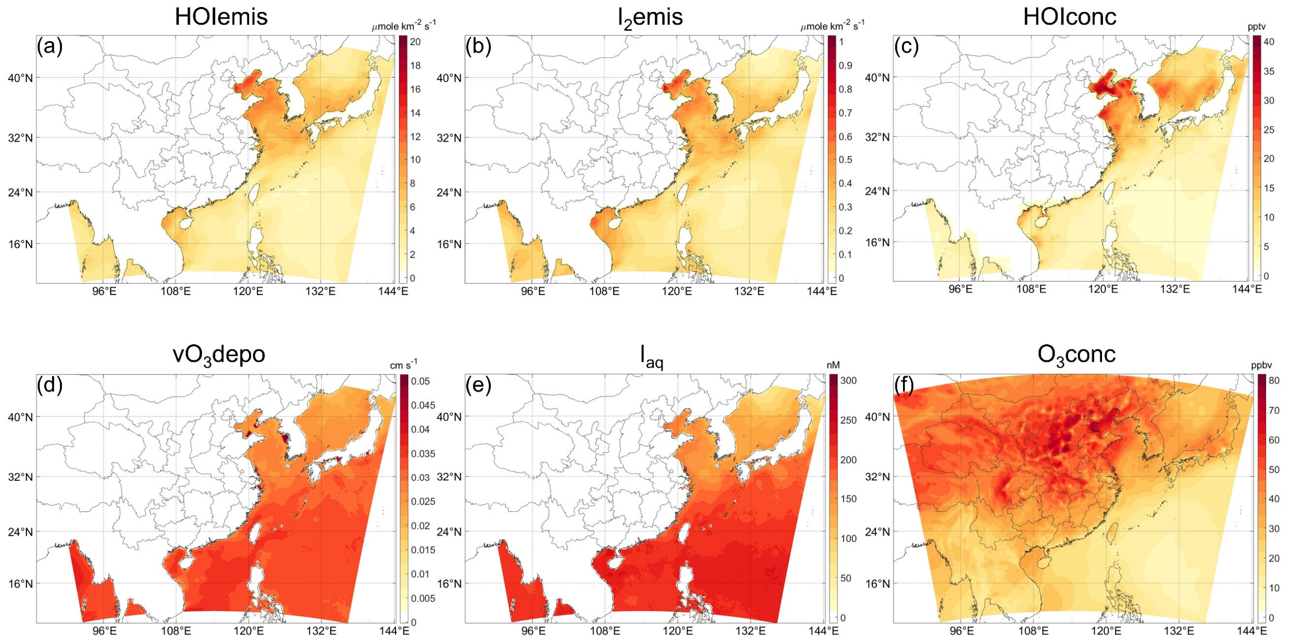

Fig. 8. Monthly average of parameters related to emission of inorganic emission in All_high case. (a) HOI emission rate, (b) I_2 emission rate, (c) HOI concentration, (d) O_3 deposition velocity over the ocean, (e) seawater iodine ion concentration, and (f) O_3 concentration. Note the different scales of (a) and (b). (d) is comparable to the values in the study of Pound et al. (2020), an annual average O_3 deposition velocity about 0.03 cm s^{-1} and in summer the deposition velocity is close to annual average in the Western Pacific, see their Figs. 2b and 3c.

The negative change of P_{OH} caused by atmospheric iodine chemistry in the Philippines Sea shown in Fig 6d is interesting and to our knowledge there is no study previously published that analyze in detail the cause of the both positive and negative impacts of iodine chemistry (e.g., Stone et al., 2018). To investigate the factors driving the spatial variability of iodine-induced OH production, the monthly averaged values of the parameters related to emission of inorganic emission in All_high case are plotted in Fig. 8. As expected, the pattern of ΔP_{OH} do not coincide with the pattern of seawater iodine concentration (Fig. 8e) and the ozone deposition velocity (Fig. 8d), which decrease with latitude due to the increase in temperature. The location of the area of negative ΔP_{OH} roughly coincides with the area with lower emission rate of HOI (Fig. 8a), I_2 emission (Fig. 8b), HOI concentration (Fig. 8c), and O_3 concentration (Fig. 8f). The positive changes of P_{OH} could be directly attributable to the effect of iodine chemical cycling. What are the causes of the negative change of P_{OH}? To figure out the causes, we conduct sensitivity simulations to analyze the contribution of I_2/HOI emissions and O_3 concentration on the negative ΔP_{OH}.

First, we find that the emission of HOI as a primary OH source is not the cause. The PA results show that the emission rate of HOI is much smaller than that of HOI cycling rate (Fig.S8a,b). Moreover, the change of P_{OH_HOX} by replacing direct HOI emission with an equivalent amount of I_2 using the emission scaling technique developed by Murphy et al. (2021) is relatively ignorable (Fig. S8c), and even without direct HOI emission (i.e., replaced by I_2) there can be also negative P_{OH} in the area (Fig. S8d). Second, we show that the lower inorganic iodine (emitted as HOI or I_2) in the Philippine Sea is probably not the direct cause of the negative ΔP_{OH} there by two sensitivity runs. When reducing HOI/I_2 emission rates by 50% using the emission scaling technique developed by Murphy et al. (2021), the area of negative ΔP_{OH} does not increase because value of ΔP_{OH} is actually increased in the Philippine Sea (Fig. S9a,b), indicating that fewer available iodine atom does not necessarily enlarge the area of negative ΔP_{OH} in the Philippines Sea. Furthermore, when we change the HOI/I_2 emission over Philippine Sea by setting HOI/I_2 emission rates in the domain to constants ($6.86=5000/27^2$ μmole km^{-2} s^{-1} for HOI, and 1/20 of HOI for I_2, see Fig. 8a,b for comparison) which are between the emission rates in the Philippine Sea and that in the Bohai Sea, the pattern of ΔP_{OH} is very similar to that in the InorgI_chem case (Figs. S9e and 7e). This similarity strongly suggests that the emission rate distribution of inorganic iodine is also not important to determine the positive-or-negative pattern of iodine-chemistry-induced ΔP_{OH}. In the regions other than the Philippine Sea, P_{OH} generally increases/decreases with the increase/decrease of HOI/I_2 emission rate (compare Figs. S9c and S9b, and S9f and S9e), but in the Philippine Sea, where the negative ΔP_{OH} appears, the trend is opposite. Is this because the complex interaction between the marine iodine chemistry and the continental atmospheric pollution leading the special negative ΔP_{OH} in the Philippine Sea? Third, to investigate whether it is true, we increase O_3 concentration downwind the Philippines (Fig. S10a) by increasing NO*x* and VOCs emission rates in the Philippines by a factor of five. The iodine-chemistry-induced change of P_{OH} becomes negative in most of the Philippines Sea (Fig. S10c). More specifically, when increasing O_3 concentration downwind the Philippines, the further change of the iodine-chemistry-induced ΔP_{OH} has a striking characteristic over the ocean (Fig. S10c): positive close to the source on the island but negative farther away. This characteristic results from the different distribution of P_{OH_O1D} (Fig. S10d) and P_{OH_HOX} (Fig. S10e) along the O_3 plume: the former relatively evenly distributed while the latter weakening gradually along the plume. The decrease of P_{OH_O1D} along the O_3 plume is due to the O_3 consumption via R1, and the evenly distribution, which is different from the O_3 distribution (Fig. S10a), indicates the sufficient O_3 is available for R1 and there is accumulated O_3 depletion along the transport path. In contrast, the gradually decrease of ΔP_{OH_HOX} along the plume path is similar to the O_3 distribution (Fig. S10a), because HOI cycle is essentially local due to the very high cycling rate of HOI, leading to the local impact of P_{OH_HOX}. To confirm the impact of the "upwind O_3-depletion" by iodine (R1) in the Philippine Sea, we illustrate in Fig. 9c the ratio of O_3 concentration decrease to O_3 local loss rate, to characterize qualitatively the contribution of the "upwind O_3-depletion" by iodine (R1) in the domain. Indeed, the ratio has maxima in the Philippine Sea where the iodine-chemistry-induced ΔP_{OH} are negative (Fig. 7e), indicating an "excessive" decrease of O_3 compared to its local consumption in the area (Fig. 9), which can only be explained by the gradually enhancement of "upwind O_3-depletion" by iodine along the plume paths (in InorgI_chem case, compared to BASE case, iodine atom is the only significant consumer of O_3).

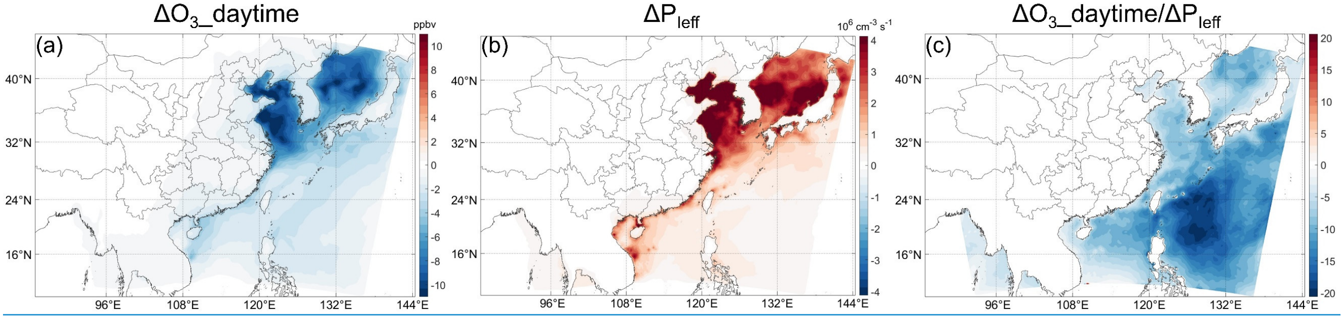

Fig. 9. Iodine chemistry induced change of (a) daytime (LT 8:00–16:00) O_3 concentration and (b) production rate of effective iodine atom (iodine atom that can consume O_3, including all reactions that can produce iodine atom except IO photolysis which will produce O and reactions which produce NO_2), ≈ O_3 loss rate by local iodine chemistry. (c) The ratio between (a) and (b), only for qualitative illustration. The large negative values in the Philippine Sea of (c) indicates the large "excessive" decrease of O_3 compared to its local consumption.

Therefore, in the Philippine Sea, the negative iodine-chemistry-induced ΔP_{OH} is probably caused by the gradually enhancement of "upwind O_3-depletion" by iodine along the plume paths, which results in the higher contribution of accumulated O_3 depletion and therefor less contribution of local O_3 destruction (and OH production) reactions. Excluding the importance of HOI/I_2 emission rates distribution (Fig. S9), only two parameters are possible to influence the effect of accumulated "upwind O_3-depletion by iodine", the O_3 concentration upwind and the path length (over ocean) of transport of air mass, because accumulation depends both on speed and time of accumulation. The former is easier to conceive and illustrate, and the lower value of it in the Philippine Sea (Fig. 8f) indeed roughly coincide with the negative (Fig. 7e). However, as shown by the case with increased O_3 concentration downwind the Philippines that P_{OH} is not increased by increased O_3 concentration in general (Fig. S10), suggesting that the second parameter is more important. Unfortunately, it is difficult to quantify the path length of transport of air mass, and the decisive evidence is therefore absent here.

As such, we can conclude that whether the iodine-chemistry-induced ΔP_{OH} is negative or positive over the ocean is determined by the relative abundance of O_3 and the transport length of O_3-abundant air mass before it reaches the focused location, and the latter is possibly more important. In the Philippine Sea area, O_3 concentration is low, and O_3 is generally transported from the Philippines and the southeast boundaries that indicate the possibility to experience significant consumption by iodine when the "fresh" O_3 arrive there (see Fig. S10c as an example); therefore, it is possible for the dominant effect of "upwind O_3-depletion by iodine" along the plume paths, which result in an overall negative iodine-chemistry-induced ΔP_{OH}. On the other hand, the O_3 in the Chinese seas and Sea of Japan have different sources (local sources in the ocean and transported from the nearby land) and have high concentration, possibly resulting in a shorter transport path length before the air mass arrive and therefore a relatively prominent effect of iodine cycling and a relatively week effect of "upwind O_3-depletion by iodine" along the plume paths, which results in an overall positive iodine-chemistry-induced ΔP_{OH}.

3.4.4 Summary of the influences of the factors

In summary, we can conclude that the marine-emitted halogen species can result in a complicated change of P_{OH} in East Asia (Fig. 2), with negative ΔP_{OH} in ~~the middle area~~most areas of the ocean while positive in the north and south parts especially in the nearshore areas. IRR analysis results show that the changes of photolysis of O_3 and HOX, and the reaction HO_2+Y are the main contributors to ΔP_{OH} (Fig. 3). These three pathways are influenced by different factors related to different species. For the photolysis of O_3, both SSA and iodine can significantly decrease it, but with different mechanisms. SSA mainly influence the photolysis through a physical factor, by extinction solar radiation, which in turn can decrease both $J(O^1D)$ and O_3 concentration. Inorganic iodine can only decrease O_3 concentration, through the enhanced O_3 deposition and the atmospheric destruction of O_3, but to a much larger extent than that caused by SSA. For the photolysis of HOX, only the cycling of HOI has a significant contribution. For the conversion of HO_2 to OH, IO will compete with NO and O_3 to consume HO_2, resulting a significant decrease of the conversion; while the SSA can also lead to a decrease of the conversion, probably through more complicated feedbacks.

By influencing the strengths of the three pathways, these factors determine the pattern of the net ΔP_{OH}. More specifically, the basic pattern of ΔP_{OH}, with the largest relative decrease in the Philippine Sea (Fig. 2b), is controlled by the atmospheric iodine chemistry which shows negative ΔP_{OH} value only there (Fig. 6d), while the other marine areas can be roughly seen as the competition between the relatively evenly distributed negative ΔP_{OH} and the positive iodine-chemistry-induced ΔP_{OH}. In the Philippine Sea, the O_3 concentration decrease more than that is consumed locally, resulting in an "excessive" decrease of O_3 and therefore negative ΔP_{OH}. ~~Other areas show more influence of local chemical consumption of O_3 (Fig. S8e), which is generally accompanied by the more efficient HOI cycling (and OH production) (Fig. S8c), and therefore positive iodine-chemistry-induced ΔP_{OH}. The HOI cycling is very strong in the northern seas (Fig. 7h), which is probably due to the higher levels of relevant gases such as O_3 that would result in high emission rates of inorganic iodine (Carpenter et al., 2013) and would enhance the cycling of reactions R1–R3~~The excessive decrease of O_3 illustrates the effect of accumulated "upwind O_3-depletion by iodine", which results from the high concentration of O_3 and possibly long transport path length of O_3-abundant air mass before reaching the location, and the low emission rates of HOI/I_2 are not important. Other areas show more influence of local chemical consumption of O_3 (Fig. 9c), which is generally accompanied by the more efficient HOI cycling (and OH production), and therefore positive iodine-chemistry-induced ΔP_{OH}.

In the Bohai Sea, the chemistry of SSA Cl also plays a role in increasing P_{OH}, probably due to the higher concentrations of NO_x (for Cl activation) and VOCs (for RO_2 production) there. Similarly, the NCP also shows noticeable contribution of SSA Cl chemistry on ΔP_{OH}, but the impact is shaded by the negative contribution of SSA extinction effect on ΔP_{OH} (Figs. 4a, 5a,e).

3.5 Limitations

There are several limitations in our investigation. Our results rely much on the ~~reliability of~~ current halogen chemistry in CTMs, which is still under development. ~~Recent model studies focused on the heterogeneous reactions of HOBr which can solve the problem of excessive BrO caused by debromination in GEOS-Chem~~ (Zhu et al., 2019;Wang et al., 2021)~~. But in our study, BrO is not excessive when including debromination and the contribution of Br chemistry to ΔP_{OH} is small, indicating the update of HOBr chemistry may not be critical to our results.~~ The uncertainty in the Cl activation and its oxidations of VOCs may have larger impacts, but the recent update of N_2O_5 uptake in China does not improve Cl chemistry significantly (Dai et al., 2020), and due to the complexity of VOCs reactions, there are very few studies focused on the updates of Cl-VOCs chemistry. More studies on the parameterization of Cl activation and following Cl-VOCs reactions are needed. Recent GEOS-Chem studies improved the uptake of HOBr substantially, but the two major revisions have opposite effects on BrO: increasing HOBr uptake by using more sophisticated parameterizations (Schmidt et al., 2016) and decreasing Br_2 yield by adding competition reactions of HOBr with S(IV) (Zhu et al., 2019;Chen et al., 2017;Wang et al., 2021). The uptake of HOBr in our study is simply parameterized with a constant reactive uptake coefficient 0.1 (Sarwar et al., 2019), which may result in a lower debromination rate. However, since Br chemistry influences OH mainly through the consumption of O_3 (Stone et al., 2018), the constraining on modelled BrO is sufficient for our purpose. As shown in 3.1, modelled BrO is comparable to previous studies (Zhu et al., 2019), indicating the update of HOBr chemistry may not be critical to our results, but more measurements of BrO with seasonality information are needed for further evaluation of the impacts of Br chemistry. Furthermore, the fact that excluding of SSA debromination through HOBr+Br^- reaction in several previous GEOS-Chem studies (Sherwen et al., 2016;Stone et al., 2018;Schmidt et al., 2016) does not decrease BrO burden (Zhu et al., 2019) indicates that there are more complicated interactions between different reactive bromine species (Br_y) and more careful check are needed. The largest limitation comes from the iodine chemistry because it is the main contributor to the change of P_{OH} through different pathways. A recent observation study reported a much faster uptake of HOI and release of ICl and IBr (Tham et al., 2021), which may have large impacts on the cycling of HOI. In particular, since the photolysis of ICl and IBr is faster than that of HOI, iodine atom would be more rapidly recycled and O_3 would be more efficiently consumed (Tham et al., 2021) but without producing OH. At the same time, OH production from HOI photolysis would be slower since HOI is more efficiently removed from the system. As a result, the impact of iodine chemistry on OH would be more negative (Kanaya et al., 2002). Related to the iodine chemistry, the enhancement of O_3 deposition to the ocean is also not satisfactorily parameterized (Loades et al., 2020;Luhar et al., 2018;Pound et al., 2020). Therefore, the incomplete halogen chemistry may limit the representativeness of our results but probably result in a larger impact of halogen chemistry on OH.

~~Another limitation is the absence of the uptake of HO_2 by aerosols in CMAQ. The emission of SSA will introduce a large number of particles into the atmosphere, which would obviously influence the uptake of HO_2. However, current knowledge about the uptake coefficient of HO_2 (γ_{HO2}) is rare and a constant 0.2 is generally used in CTMs (Song et al., 2020;Zhou et al.,~~

~~2020;Zhou et al., 2021). With the lack of experiment- and/or observation-constrained parameterizations of the uptake of HO_2 by SSA, a constant γ_{HO2} and a large number of SSA particles may introduce large uncertainty in evaluating the impact on P_{OH} of SSA's uptake of HO_2. Therefore, we do not include the uptake of HO_2 in CMAQ (as default), but the limitation may be considered in further investigations when more are known about the HO_2 uptake.~~

4. Conclusions

To examine the ~~mass interaction~~impacts of gas/particle exchange between ocean and atmosphere on the regional air oxidation capacity, we explore the impact of marine-emitted halogen species on atmospheric OH in East Asia in summer. The net ΔP_{OH} caused by all marine-emitted halogen species has both positive and negative signs in the marine atmosphere and the positive ΔP_{OH} appears mainly at nearshore areas. The monthly P_{OH} is generally decreased over the ocean with maxima of 10–15% in the Philippine Sea, but is increased in many nearshore areas, with maxima of 7–9% in the Bohai Sea. In the coastal areas of southern China, the monthly change of P_{OH} could also decrease 3–5% in the Greater Bay Area, but ~~with a daytime~~the hourly ~~maximum~~values can decrease over 30~~%.~~% in the daytime. These results indicate a notable impact of marine-emitted halogens on atmospheric oxidation capacity~~.~~, which could have significant implication in the lifetime of long-lived species such as CH_4 (one of the major greenhouse gases) in long-term and amount of air pollutants such as O_3 in the episodic events.

IRR analysis show that the net effect of ΔP_{OH} is controlled by the competitions of three main pathways through different halogen species, while the contributions of other pathways are minor. In additional to the two well-known pathways involving the changes of the photolysis of O_3 and HOX, the competition on HO_2 of XO with NO and O_3 also significantly changes the OH production rate. These three main pathways are influenced by different factors that are related to different halogen species. SSA and inorganic iodine gases have the most significant impacts on P_{OH}. In this study, in additional to the chemical impacts, the physical impacts of the marine-emitted halogens on OH are also explicitly and quantitatively examined. More specifically, ~~Both~~ SSA and inorganic iodine decrease P_{OH} through physical processes including the extinction effect of SSA and the enhancement of ozone deposition by oceanic iodine, while generally ~~increase~~ increasing P_{OH} through chemical processes among which the Cl (from SSA) and inorganic iodine chemistry are the most important. The physical impacts are quite comparable to the chemical impacts. In the continent, SSA is the controlling species and its extinction effect leads to the negative ΔP_{OH} in the southern China. While in the ocean atmosphere, ~~the controlling species are~~ inorganic iodine gases ~~and~~are more important as the complicated iodine chemistry determines the basic pattern of ΔP_{OH}. It is the competition between iodine's enhancing effect on the conversion of HO_2 to OH and iodine's decreasing effect on OH production from O_3 that determines the sign of iodine-chemistry-induced ΔP_{OH}. The relative strengths of these two opposing effects are controlled by the O_3 concentration and the transport path length of O_3-abundant air mass over the ocean, which determine the relative importance of accumulated "upwind O_3-depletion by iodine" (negative effect) compared to local iodine cycle (positive effect).

Although the uncertainties in estimating the emission rates of different halogen species could influence on the magnitude and even the distribution of the halogen-induced change of P_{OH}, the ~~significant impact of the marine-emitted halogen species on the oceanic OH radical and the potential impact on the coastal atmosphere oxidation in the episodic events have been clearly revealed. In addition, the~~ response of the main contributors of P_{OH} to the individual species and pathway and their influencing factors have been ~~identified~~quantified, which explains the spatial variability of halogen-induced ~~change of~~ ΔP_{OH} over East Asia and also can be applied in other circumstances (e.g., different domains, regions, and emission rates).

Data availability

Hourly O_3 concentration data could be obtained from https://quotsoft.net/air/ (Ministry of Environmental Protection of China). NCEP datasets are available at https://rda.ucar.edu. The chl-*a* data can be downloaded from the merged products of the GlobColour data set (http://globcolour.info).

Author contribution

YL designed the study and wrote the manuscript. SF run the simulations, conducted analyses, and wrote the manuscript.

Competing interests

The authors declare that they have no conflict of interest.

Acknowledgment

We thank the editor and three anonymous reviewers for their valuable comments. This research was funded by Guangdong Basic and Applied Basic Research Fund Committee (2020B1515130003)，Key Special Project for Introduced Talents Team of Southern Marine Science and Engineering Guangdong Laboratory (Guangzhou), grant number GML2019ZD0210; National Natural Science Foundation of China, grant number 41961160728, 41575106, 42105124; Shenzhen Science and Technology Program, grant number KQTD20180411143441009, Key-Area Research and Development Program of Guangdong Province, grant number 2020B1111360001, Shenzhen Key Laboratory Foundation (ZDSYS20180208184349083), the Guangdong Province Science and Technology Planning Project of China, grant number 2017A050506003, Center for Computational Science and Engineering at Southern University of Science and Technology.~~This work was supported by the National Natural Science Foundation of China (Grant no. 41961160728), the Guangdong Province Science and Technology Planning Project of China (Grant no. 2017A050506003), National Natural Science Foundation of China (Grant no. 41575106), Shenzhen Science and Technology Program (KQTD20180411143441009), Key Special Project for Introduced Talents Team of Southern Marine Science and~~

~~Engineering Guangdong Laboratory (Guangzhou) (GML2019ZD0210), Guangdong Basic and Applied Basic Research Fund Committee (2020B1515130003), Key-Area Research and Development Program of Guangdong Province (2020B1111360001), Shenzhen Key Laboratory Foundation (ZDSYS20180208184349083), Center for Computational Science and Engineering at Southern University of Science and Technology.~~

References

Appel, K. W., Bash, J. O., Fahey, K. M., Foley, K. M., Gilliam, R. C., Hogrefe, C., Hutzell, W. T., Kang, D. W., Mathur, R., Murphy, B. N., Napelenok, S. L., Nolte, C. G., Pleim, J. E., Pouliot, G. A., Pye, H. O. T., Ran, L. M., Roselle, S. J., Sarwar, G., Schwede, D. B., Sidi, F. I., Spero, T. L., and Wong, D. C.: The Community Multiscale Air Quality (CMAQ) model versions 5.3 and 5.3.1: system updates and evaluation, Geoscientific Model Development, 14, 2867-2897, 10.5194/gmd-14-2867-2021, 2021.

Archibald, A. T., Cooke, M. C., Utembe, S. R., Shallcross, D. E., Derwent, R. G., and Jenkin, M. E.: Impacts of mechanistic changes on HOx formation and recycling in the oxidation of isoprene, Atmospheric Chemistry and Physics, 10, 8097-8118, 10.5194/acp-10-8097-2010, 2010.

Barthel, S., Tegen, I., and Wolke, R.: Do new sea spray aerosol source functions improve the results of a regional aerosol model?, Atmospheric Environment, 198, 265-278, 10.1016/j.atmosenv.2018.10.016, 2019.

Bates, K. H., and Jacob, D. J.: A new model mechanism for atmospheric oxidation of isoprene: global effects on oxidants, nitrogen oxides, organic products, and secondary organic aerosol, Atmospheric Chemistry and Physics, 19, 9613-9640, 10.5194/acp-19-9613-2019, 2019.

Carpenter, L. J., MacDonald, S. M., Shaw, M. D., Kumar, R., Saunders, R. W., Parthipan, R., Wilson, J., and Plane, J. M. C.: Atmospheric iodine levels influenced by sea surface emissions of inorganic iodine, Nature Geoscience, 6, 108-111, 10.1038/ngeo1687, 2013.

Carpenter, L. J., Chance, R. J., Sherwen, T., Adams, T. J., Ball, S. M., Evans, M. J., Hepach, H., Hollis, L. D. J., Hughes, C., Jickells, T. D., Mahajan, A., Stevens, D. P., Tinel, L., and Wadley, M. R.: Marine iodine emissions in a changing world, Proceedings of the Royal Society a-Mathematical Physical and Engineering Sciences, 477, 10.1098/rspa.2020.0824, 2021.

Chance, R., Baker, A. R., Carpenter, L., and Jickells, T. D.: The distribution of iodide at the sea surface, Environmental Science-Processes & Impacts, 16, 1841-1859, 10.1039/c4em00139g, 2014.

Chang, W. N., Heikes, B. G., and Lee, M. H.: Ozone deposition to the sea surface: chemical enhancement and wind speed dependence, Atmospheric Environment, 38, 1053-1059, 10.1016/j.atmosenv.2003.10.050, 2004.

Chen, Q., Schmidt, J. A., Shah, V., Jaegle, L., Sherwen, T., and Alexander, B.: Sulfate production by reactive bromine: Implications for the global sulfur and reactive bromine budgets, Geophysical Research Letters, 44, 7069-7078, 10.1002/2017gl073812, 2017.

Dai, J. N., Liu, Y. M., Wang, P., Fu, X., Xia, M., and Wang, T.: The impact of sea-salt chloride on ozone through heterogeneous reaction with N_2O_5 in a coastal region of south China, Atmospheric Environment, 236, 10.1016/j.atmosenv.2020.117604, 2020.

Emery, C., Liu, Z., Russell, A. G., Odman, M. T., Yarwood, G., and Kumar, N.: Recommendations on statistics and benchmarks to assess photochemical model performance, Journal of the Air & Waste Management Association, 67, 582-598, 10.1080/10962247.2016.1265027, 2017.

Engel, A., Rigby, M., Burkholder, J., Fernandez, R., Froidevaux, L., Hall, B., Hossaini, R., Saito, T., Vollmer, M., and Yao, B. J. S. A. o. O. D.: Update on Ozone-Depleting Substances (ODSs) and Other Gases of Interest to the Montreal Protocol, in: Scientific Assessment of Ozone Depletion: 2018, 1-87, 2019.

Fairall, C. W., Helmig, D., Ganzeveld, L., and Hare, J.: Water-side turbulence enhancement of ozone deposition to the ocean, Atmospheric Chemistry and Physics, 7, 443-451, 10.5194/acp-7-443-2007, 2007.

Fan, S., Li, Y., and Liu, C.: Are Environmentally Friendly Fireworks Really "Green" for Air Quality? A Study from the 2019 National Day Fireworks Display in Shenzhen, Environmental Science & Technology, 55, 3520-3529, 10.1021/acs.est.0c03521, 2021.

Fittschen, C., Al Ajami, M., Batut, S., Ferracci, V., Archer-Nicholls, S., Archibald, A. T., and Schoemaecker, C.: ROOOH: a missing piece of the puzzle for OH measurements in low-NO environments?, Atmospheric Chemistry and Physics, 19, 349-362, 10.5194/acp-19-349-2019, 2019.

Fuchs, H., Hofzumahaus, A., Rohrer, F., Bohn, B., Brauers, T., Dorn, H. P., Haseler, R., Holland, F., Kaminski, M., Li, X., Lu, K., Nehr, S., Tillmann, R., Wegener, R., and Wahner, A.: Experimental evidence for efficient hydroxyl radical regeneration in isoprene oxidation, Nature Geoscience, 6, 1023-1026, 10.1038/ngeo1964, 2013.

Gantt, B., Kelly, J. T., and Bash, J. O.: Updating sea spray aerosol emissions in the Community Multiscale Air Quality (CMAQ) model version 5.0.2, Geoscientific Model Development, 8, 3733-3746, 10.5194/gmd-8-3733-2015, 2015.

Gao, J., Li, Y., Zhu, B., Hu, B., Wang, L., and Bao, F.: What have we missed when studying the impact of aerosols on surface ozone via changing photolysis rates?, Atmospheric Chemistry and Physics, 20, 10831-10844, 10.5194/acp-20-10831-2020, 2020a.

Gao, M., Gao, J. H., Zhu, B., Kumar, R., Lu, X., Song, S. J., Zhang, Y. Z., Jia, B. X., Wang, P., Beig, G. R., Hu, J. L., Ying, Q., Zhang, H. L., Sherman, P., and McElroy, M. B.: Ozone pollution over China and India: seasonality and sources, Atmospheric Chemistry and Physics, 20, 4399-4414, 10.5194/acp-20-4399-2020, 2020b.

Gong, S. L.: A parameterization of sea-salt aerosol source function for sub- and super-micron particles, Global Biogeochemical Cycles, 17, 10.1029/2003gb002079, 2003.

Großmann, K., Friess, U., Peters, E., Wittrock, F., Lampel, J., Yilmaz, S., Tschritter, J., Sommariva, R., von Glasow, R., Quack, B., Kruger, K., Pfeilsticker, K., and Platt, U.: Iodine monoxide in the Western Pacific marine boundary layer, Atmospheric Chemistry and Physics, 13, 3363-3378, 10.5194/acp-13-3363-2013, 2013.

Grythe, H., Strom, J., Krejci, R., Quinn, P., and Stohl, A.: A review of sea-spray aerosol source functions using a large global set of sea salt aerosol concentration measurements, Atmospheric Chemistry and Physics, 14, 1277-1297, 10.5194/acp-14-1277-2014, 2014.

Guenther, A. B., Jiang, X., Heald, C. L., Sakulyanontvittaya, T., Duhl, T., Emmons, L. K., and Wang, X.: The Model of Emissions of Gases and Aerosols from Nature version 2.1 (MEGAN2.1): an extended and updated framework for modeling biogenic emissions, Geoscientific Model Development, 5, 1471-1492, 10.5194/gmd-5-1471-2012, 2012.

Hofzumahaus, A., Rohrer, F., Lu, K. D., Bohn, B., Brauers, T., Chang, C. C., Fuchs, H., Holland, F., Kita, K., Kondo, Y., Li, X., Lou, S. R., Shao, M., Zeng, L. M., Wahner, A., and Zhang, Y. H.: Amplified Trace Gas Removal in the Troposphere, Science, 324, 1702-1704, 10.1126/science.1164566, 2009.

Hu, L., Jacob, D. J., Liu, X., Zhang, Y., Zhang, L., Kim, P. S., Sulprizio, M. P., and Yantosca, R. M.: Global budget of tropospheric ozone: Evaluating recent model advances with satellite (OMI), aircraft (IAGOS), and ozonesonde observations, Atmospheric Environment, 167, 323-334, 10.1016/j.atmosenv.2017.08.036, 2017.

Huang, Y., Lu, X., Fung, J. C. H., Sarwar, G., Li, Z., Li, Q., Saiz-Lopez, A., and Lau, A. K. H.: Effect of bromine and iodine chemistry on tropospheric ozone over Asia-Pacific using the CMAQ model, Chemosphere, 262, 127595-127595, 10.1016/j.chemosphere.2020.127595, 2020.

Inamdar, S., Tinel, L., Chance, R., Carpenter, L. J., Sabu, P., Chacko, R., Tripathy, S. C., Kerkar, A. U., Sinha, A. K., Bhaskar, P. V., Sarkar, A., Roy, R., Sherwen, T., Cuevas, C., Saiz-Lopez, A., Ram, K., and Mahajan, A. S.: Estimation of reactive inorganic iodine fluxes in the Indian and Southern Ocean marine boundary layer, Atmospheric Chemistry and Physics, 20, 12093-12114, 10.5194/acp-20-12093-2020, 2020.

Jaeglé, L., Quinn, P. K., Bates, T. S., Alexander, B., and Lin, J. T.: Global distribution of sea salt aerosols: new constraints from in situ and remote sensing observations, Atmospheric Chemistry and Physics, 11, 3137-3157, 10.5194/acp-11-3137-2011, 2011.

Kanaya, Y., Yokouchi, Y., Matsumoto, J., Nakamura, K., Kato, S., Tanimoto, H., Furutani, H., Toyota, K., and Akimoto, H.: Implications of iodine chemistry for daytime HO2 levels at Rishiri Island, Geophysical Research Letters, 29, 10.1029/2001gl014061, 2002.

Kelly, J. T., Bhave, P. V., Nolte, C. G., Shankar, U., and Foley, K. M.: Simulating emission and chemical evolution of coarse sea-salt particles in the Community Multiscale Air Quality (CMAQ) model, Geoscientific Model Development, 3, 257-273, 10.5194/gmd-3-257-2010, 2010.

Koenig, T. K., Volkamer, R., Baidar, S., Dix, B., Wang, S. Y., Anderson, D. C., Salawitch, R. J., Wales, P. A., Cuevas, C. A., Fernandez, R. P., Saiz-Lopez, A., Evans, M. J., Sherwen, T., Jacob, D. J., Schmidt, J., Kinnison, D., Lamarque, J. F., Apel, E. C., Bresch, J. C., Campos, T., Flocke, F. M., Hall, S. R., Honomichl, S. B., Hornbrook, R., Jensen, J. B., Lueb, R., Montzka, D. D., Pan, L. L., Reeves, J. M., Schauffler, S. M., Ullmann, K., Weinheimer, A. J., Atlas, E. L., Donets, V., Navarro, M. A., Riemer, D., Blake, N. J., Chen, D. X., Huey, L. G., Tanner, D. J., Hanisco, T. F., and Wolfe, G. M.: BrO and inferred Br-y profiles over the western Pacific: relevance of inorganic bromine sources and a Br-y minimum in the aged tropical tropopause layer, Atmospheric Chemistry and Physics, 17, 15245-15270, 10.5194/acp-17-15245-2017, 2017.

Le Breton, M., Bannan, T. J., Shallcross, D. E., Khan, M. A., Evans, M. J., Lee, J., Lidster, R., Andrews, S., Carpenter, L. J., Schmidt, J., Jacob, D., Harris, N. R. P., Bauguitte, S., Gallagher, M., Bacak, A., Leather, K. E., and Percival, C. J.: Enhanced ozone loss by active inorganic bromine chemistry in the tropical troposphere, Atmospheric Environment, 155, 21-28, 10.1016/j.atmosenv.2017.02.003, 2017.

Lelieveld, J., Butler, T. M., Crowley, J. N., Dillon, T. J., Fischer, H., Ganzeveld, L., Harder, H., Lawrence, M. G., Martinez, M., Taraborrelli, D., and Williams, J.: Atmospheric oxidation capacity sustained by a tropical forest, Nature, 452, 737-740, 10.1038/nature06870, 2008.

Lennartz, S. T., Krysztofiak, G., Marandino, C. A., Sinnhuber, B. M., Tegtmeier, S., Ziska, F., Hossaini, R., Kruger, K., Montzka, S. A., Atlas, E., Oram, D. E., Keber, T., Bonisch, H., and Quack, B.: Modelling marine emissions and atmospheric distributions of halocarbons and dimethyl sulfide: the influence of prescribed water concentration vs. prescribed emissions, Atmospheric Chemistry and Physics, 15, 11753-11772, 10.5194/acp-15-11753-2015, 2015.

Li, Q. Y., Borge, R., Sarwar, G., de la Paz, D., Gantt, B., Domingo, J., Cuevas, C. A., and Saiz-Lopez, A.: Impact of halogen chemistry on summertime air quality in coastal and continental Europe: application of the CMAQ model and implications for regulation, Atmospheric Chemistry and Physics, 19, 15321-15337, 10.5194/acp-19-15321-2019, 2019.

Li, Q. Y., Badia, A., Wang, T., Sarwar, G., Fu, X., Zhang, L., Zhang, Q., Fung, J., Cuevas, C. A., Wang, S. S., Zhou, B., and Saiz-Lopez, A.: Potential Effect of Halogens on Atmospheric Oxidation and Air Quality in China, Journal of Geophysical Research: Atmospheres, 125, 10.1029/2019jd032058, 2020.

Liu, S., Liu, C.-C., Froyd, K. D., Schill, G. P., Murphy, D. M., Bui, T. P., Dean-Day, J. M., Weinzierl, B., Dollner, M., Diskin, G. S., Chen, G., and Gao, R.-S.: Sea spray aerosol concentration modulated by sea surface temperature, Proceedings of the National Academy of Sciences, 118, e2020583118, 10.1073/pnas.2020583118, 2021.

Liu, Y. L., Nie, W., Xu, Z., Wang, T. Y., Wang, R. X., Li, Y. Y., Wang, L., Chi, X. G., and Ding, A. J.: Semi-quantitative understanding of source contribution to nitrous acid (HONO) based on 1 year of continuous observation at the SORPES station in eastern China, Atmospheric Chemistry and Physics, 19, 13289-13308, 10.5194/acp-19-13289-2019, 2019.

Loades, D. C., Yang, M. X., Belli, T. G., Vaughan, A. R., Pound, R. J., Metzger, S., Lee, J. D., and Carpenter, L. J.: Ozone deposition to a coastal sea: comparison of eddy covariance observations with reactive air-sea exchange models, Atmospheric Measurement Techniques, 13, 6915-6931, 10.5194/amt-13-6915-2020, 2020.

Lu, K. D., Guo, S., Tan, Z. F., Wang, H. C., Shang, D. J., Liu, Y. H., Li, X., Wu, Z. J., Hu, M., and Zhang, Y. H.: Exploring atmospheric free-radical chemistry in China: the self-cleansing capacity and the formation of secondary air pollution, National Science Review, 6, 579-594, 10.1093/nsr/nwy073, 2019a.

Lu, X., Zhang, L., Chen, Y., Zhou, M., Zheng, B., Li, K., Liu, Y., Lin, J., Fu, T. M., and Zhang, Q.: Exploring 2016–2017 surface ozone pollution over China: source contributions and meteorological influences, Atmospheric Chemistry and Physics, 19, 8339-8361, 10.5194/acp-19-8339-2019, 2019b.

Luhar, A. K., Galbally, I. E., Woodhouse, M. T., and Thatcher, M.: An improved parameterisation of ozone dry deposition to the ocean and its impact in a global climate-chemistry model, Atmospheric Chemistry and Physics, 17, 3749-3767, 10.5194/acp-17-3749-2017, 2017.

Luhar, A. K., Woodhouse, M. T., and Galbally, I. E.: A revised global ozone dry deposition estimate based on a new two-layer parameterisation for air-sea exchange and the multi-year MACC composition reanalysis, Atmospheric Chemistry and Physics, 18, 4329-4348, 10.5194/acp-18-4329-2018, 2018.

MacDonald, S. M., Martin, J. C. G., Chance, R., Warriner, S., Saiz-Lopez, A., Carpenter, L. J., and Plane, J. M. C.: A laboratory characterisation of inorganic iodine emissions from the sea surface: dependence on oceanic variables and parameterisation for global modelling, Atmospheric Chemistry and Physics, 14, 5841-5852, 10.5194/acp-14-5841-2014, 2014.

Mahajan, A. S., Li, Q., Inamdar, S., Ram, K., Badia, A., and Saiz-Lopez, A.: Modelling the impacts of iodine chemistry on the northern Indian Ocean marine boundary layer, Atmospheric Chemistry and Physics, 21, 8437-8454, 10.5194/acp-21-8437-2021, 2021.

Monahan, E., Spiel, D., and Davidson, K.: A model of marine aerosol generation via whitecaps and wave disruption, in: Oceanic whitecaps, Springer, 167-174, 1986.

Murphy, B. N., Nolte, C. G., Sidi, F., Bash, J. O., Appel, K. W., Jang, C., Kang, D. W., Kelly, J., Mathur, R., Napelenok, S., Pouliot, G., and Pye, H. O. T.: The Detailed Emissions Scaling, Isolation, and Diagnostic (DESID) module in the Community Multiscale Air Quality (CMAQ) modeling system version 5.3.2, Geoscientific Model Development, 14, 3407-3420, 10.5194/gmd-14-3407-2021, 2021.

Ordóñez, C., Lamarque, J. F., Tilmes, S., Kinnison, D. E., Atlas, E. L., Blake, D. R., Santos, G. S., Brasseur, G., and Saiz-Lopez, A.: Bromine and iodine chemistry in a global chemistry-climate model: description and evaluation of very short-lived oceanic sources, Atmospheric Chemistry and Physics, 12, 1423-1447, 10.5194/acp-12-1423-2012, 2012.

Ovadnevaite, J., Manders, A., de Leeuw, G., Ceburnis, D., Monahan, C., Partanen, A. I., Korhonen, H., and O'Dowd, C. D.: A sea spray aerosol flux parameterization encapsulating wave state, Atmospheric Chemistry and Physics, 14, 1837-1852, 10.5194/acp-14-1837-2014, 2014.

Pound, R. J., Sherwen, T., Helmig, D., Carpenter, L. J., and Evans, M. J.: Influences of oceanic ozone deposition on tropospheric photochemistry, Atmospheric Chemistry and Physics, 20, 4227-4239, 10.5194/acp-20-4227-2020, 2020.

Read, K. A., Mahajan, A. S., Carpenter, L. J., Evans, M. J., Faria, B. V. E., Heard, D. E., Hopkins, J. R., Lee, J. D., Moller, S. J., Lewis, A. C., Mendes, L., McQuaid, J. B., Oetjen, H., Saiz-Lopez, A., Pilling, M. J., and Plane, J. M. C.: Extensive halogen-mediated ozone destruction over the tropical Atlantic Ocean, Nature, 453, 1232-1235, 10.1038/nature07035, 2008.

Rohrer, F., Lu, K. D., Hofzumahaus, A., Bohn, B., Brauers, T., Chang, C. C., Fuchs, H., Haseler, R., Holland, F., Hu, M., Kita, K., Kondo, Y., Li, X., Lou, S. R., Oebel, A., Shao, M., Zeng, L. M., Zhu, T., Zhang, Y. H., and Wahner, A.: Maximum efficiency in the hydroxyl-radical-based self-cleansing of the troposphere, Nature Geoscience, 7, 559-563, 10.1038/ngeo2199, 2014.

Saiz-Lopez, A., and von Glasow, R.: Reactive halogen chemistry in the troposphere, Chemical Society Reviews, 41, 6448-6472, 10.1039/c2cs35208g, 2012.

Sarwar, G., Simon, H., Bhave, P., and Yarwood, G.: Examining the impact of heterogeneous nitryl chloride production on air quality across the United States, Atmospheric Chemistry and Physics, 12, 6455-6473, 10.5194/acp-12-6455-2012, 2012.

Sarwar, G., Simon, H., Xing, J., and Mathur, R.: Importance of tropospheric ClNO2 chemistry across the Northern Hemisphere, Geophysical Research Letters, 41, 4050-4058, 10.1002/2014gl059962, 2014.

Sarwar, G., Gantt, B., Schwede, D., Foley, K., Mathur, R., and Saiz-Lopez, A.: Impact of Enhanced Ozone Deposition and Halogen Chemistry on Tropospheric Ozone over the Northern Hemisphere, Environmental Science & Technology, 49, 9203-9211, 10.1021/acs.est.5b01657, 2015.

Sarwar, G., Gantt, B., Foley, K., Fahey, K., Spero, T. L., Kang, D. W., Mathur, R., Foroutan, H., Xing, J., Sherwen, T., and Saiz-Lopez, A.: Influence of bromine and iodine chemistry on annual, seasonal, diurnal, and background ozone: CMAQ simulations over the Northern Hemisphere, Atmospheric Environment, 213, 395-404, 10.1016/j.atmosenv.2019.06.020, 2019.

Schmidt, J. A., Jacob, D. J., Horowitz, H. M., Hu, L., Sherwen, T., Evans, M. J., Liang, Q., Suleiman, R. M., Oram, D. E., Le Breton, M., Percival, C. J., Wang, S., Dix, B., and Volkamer, R.: Modeling the observed tropospheric BrO background: Importance of multiphase chemistry and implications for ozone, OH, and mercury, Journal of Geophysical Research: Atmospheres, 121, 11819-11835, 10.1002/2015jd024229, 2016.

Seinfeld, J. H., and Pandis, S. N.: Atmospheric chemistry and physics: from air pollution to climate change, 3 ed., John Wiley & Sons, 2016.

Sekiya, T., Kanaya, Y., Sudo, K., Taketani, F., Iwamoto, Y., Aita, M. N., Yamamoto, A., and Kawamoto, K.: Global Bromine- and Iodine-Mediated Tropospheric Ozone Loss Estimated Using the CHASER Chemical Transport Model, Sola, 16, 220-227, 10.2151/sola.2020-037, 2020.

Sherwen, T., Schmidt, J. A., Evans, M. J., Carpenter, L. J., Grossmann, K., Eastham, S. D., Jacob, D. J., Dix, B., Koenig, T. K., Sinreich, R., Ortega, I., Volkamer, R., Saiz-Lopez, A., Prados-Roman, C., Mahajan, A. S., and Ordonez, C.: Global impacts of tropospheric halogens (Cl, Br, I) on oxidants and composition in GEOS-Chem, Atmospheric Chemistry and Physics, 16, 12239-12271, 10.5194/acp-16-12239-2016, 2016.

Sherwen, T., Chance, R. J., Tinel, L., Ellis, D., Evans, M. J., and Carpenter, L. J.: A machine-learning-based global sea-surface iodide distribution, Earth System Science Data, 11, 1239-1262, 10.5194/essd-11-1239-2019, 2019.

Simpson, W. R., Brown, S. S., Saiz-Lopez, A., Thornton, J. A., and von Glasow, R.: Tropospheric Halogen Chemistry: Sources, Cycling, and Impacts, Chemical Reviews, 115, 4035-4062, 10.1021/cr5006638, 2015.

Song, H., Chen, X., Lu, K., Zou, Q., Tan, Z., Fuchs, H., Wiedensohler, A., Moon, D. R., Heard, D. E., Baeza-Romero, M. T., Zheng, M., Wahner, A., Kiendler-Scharr, A., and Zhang, Y.: Influence of aerosol copper on HO_2 uptake: a novel parameterized equation, Atmospheric Chemistry and Physics, 20, 15835-15850, 10.5194/acp-20-15835-2020, 2020.

Stone, D., Whalley, L. K., and Heard, D. E.: Tropospheric OH and HO_2 radicals: field measurements and model comparisons, Chemical Society Reviews, 41, 6348-6404, 10.1039/c2cs35140d, 2012.

Stone, D., Sherwen, T., Evans, M. J., Vaughan, S., Ingham, T., Whalley, L. K., Edwards, P. M., Read, K. A., Lee, J. D., Moller, S. J., Carpenter, L. J., Lewis, A. C., and Heard, D. E.: Impacts of bromine and iodine chemistry on tropospheric OH and HO_2: comparing observations with box and global model perspectives, Atmospheric Chemistry and Physics, 18, 3541-3561, 10.5194/acp-18-3541-2018, 2018.

Tan, Z. F., Lu, K. D., Hofzumahaus, A., Fuchs, H., Bohn, B., Holland, F., Liu, Y. H., Rohrer, F., Shao, M., Sun, K., Wu, Y. S., Zeng, L. M., Zhang, Y. S., Zou, Q., Kiendler-Scharr, A., Wahner, A., and Zhang, Y. H.: Experimental budgets of OH, HO2, and RO2 radicals and implications for ozone formation in the Pearl River Delta in China 2014, Atmospheric Chemistry and Physics, 19, 7129-7150, 10.5194/acp-19-7129-2019, 2019.

Tham, Y. J., He, X.-C., Li, Q., Cuevas, C. A., Shen, J., Kalliokoski, J., Yan, C., Iyer, S., Lehmusjärvi, T., Jang, S., Thakur, R. C., Beck, L., Kemppainen, D., Olin, M., Sarnela, N., Mikkilä, J., Hakala, J., Marbouti, M., Yao, L., Li, H., Huang, W., Wang, Y., Wimmer, D., Zha, Q., Virkanen, J., Spain, T. G., O'Doherty, S., Jokinen, T., Bianchi, F., Petäjä, T., Worsnop, D. R., Mauldin, R. L., Ovadnevaite, J., Ceburnis, D., Maier, N. M., Kulmala, M., O'Dowd, C., Dal Maso, M., Saiz-Lopez, A., and Sipilä, M.: Direct field evidence of autocatalytic iodine release from atmospheric aerosol, Proceedings of the National Academy of Sciences, 118, e2009951118, 10.1073/pnas.2009951118, 2021.

Torseth, K., Aas, W., Breivik, K., Fjaeraa, A. M., Fiebig, M., Hjellbrekke, A. G., Myhre, C. L., Solberg, S., and Yttri, K. E.: Introduction to the European Monitoring and Evaluation Programme (EMEP) and observed atmospheric composition change during 1972-2009, Atmospheric Chemistry and Physics, 12, 5447-5481, 10.5194/acp-12-5447-2012, 2012.

Wang, X., Jacob, D. J., Eastham, S. D., Sulprizio, M. P., Zhu, L., Chen, Q. J., Alexander, B., Sherwen, T., Evans, M. J., Lee, B. H., Haskins, J. D., Lopez-Hilfiker, F. D., Thornton, J. A., Huey, G. L., and Liao, H.: The role of chlorine in global tropospheric chemistry, Atmospheric Chemistry and Physics, 19, 3981-4003, 10.5194/acp-19-3981-2019, 2019.

Wang, X., Jacob, D. J., Fu, X., Wang, T., Le Breton, M., Hallquist, M., Liu, Z. R., McDuffie, E. E., and Liao, H.: Effects of Anthropogenic Chlorine on $PM_{2.5}$ and Ozone Air Quality in China, Environmental Science & Technology, 54, 9908-9916, 10.1021/acs.est.0c02296, 2020.

Wang, X., Jacob, D. J., Downs, W., Zhai, S., Zhu, L., Shah, V., Holmes, C. D., Sherwen, T., Alexander, B., Evans, M. J., Eastham, S. D., Neuman, J. A., Veres, P. R., Koenig, T. K., Volkamer, R., Huey, L. G., Bannan, T. J., Percival, C. J., Lee, B. H., and Thornton, J. A.: Global tropospheric halogen (Cl, Br, I) chemistry and its impact on oxidants, Atmospheric Chemistry and Physics, 21, 13973-13996, 10.5194/acp-21-13973-2021, 2021.

Whalley, L. K., Furneaux, K. L., Goddard, A., Lee, J. D., Mahajan, A., Oetjen, H., Read, K. A., Kaaden, N., Carpenter, L. J., Lewis, A. C., Plane, J. M. C., Saltzman, E. S., Wiedensohler, A., and Heard, D. E.: The chemistry of OH and HO_2 radicals in the boundary layer over the tropical Atlantic Ocean, Atmospheric Chemistry and Physics, 10, 1555-1576, 10.5194/acp-10-1555-2010, 2010.

Whalley, L. K., Slater, E. J., Woodward-Massey, R., Ye, C., Lee, J. D., Squires, F., Hopkins, J. R., Dunmore, R. E., Shaw, M., Hamilton, J. F., Lewis, A. C., Mehra, A., Worrall, S. D., Bacak, A., Bannan, T. J., Coe, H., Percival, C. J., Ouyang, B., Jones, R. L., Crilley, L. R., Kramer, L. J., Bloss, W. J., Vu, T., Kotthaus, S., Grimmond, S., Sun, Y., Xu, W., Yue, S., Ren, L., Acton, W. J. F., Hewitt, C. N., Wang, X., Fu, P., and Heard, D. E.: Evaluating the sensitivity of radical chemistry and ozone formation to ambient VOCs and NOx in Beijing, Atmospheric Chemistry and Physics, 21, 2125-2147, 10.5194/acp-21-2125-2021, 2021.

Yin, S. S., Zheng, J. Y., Lu, Q., Yuan, Z. B., Huang, Z. J., Zhong, L. J., and Lin, H.: A refined 2010-based VOC emission inventory and its improvement on modeling regional ozone in the Pearl River Delta Region, China, Science of the Total Environment, 514, 426-438, 10.1016/j.scitotenv.2015.01.088, 2015.

Yu, C., Wang, Z., Xia, M., Fu, X., Wang, W., Tham, Y. J., Chen, T., Zheng, P., Li, H., Shan, Y., Wang, X., Xue, L., Zhou, Y., Yue, D., Ou, Y., Gao, J., Lu, K., Brown, S. S., Zhang, Y., and Wang, T.: Heterogeneous N_2O_5 reactions on atmospheric aerosols at four Chinese sites: improving model representation of uptake parameters, Atmospheric Chemistry and Physics, 20, 4367-4378, 10.5194/acp-20-4367-2020, 2020.

Yu, Z., and Li, Y.: Marine volatile organic compounds and their impacts on marine aerosol-A review, Science of the Total Environment, 768, 10.1016/j.scitotenv.2021.145054, 2021.

Zheng, J. Y., Zhang, L. J., Che, W. W., Zheng, Z. Y., and Yin, S. S.: A highly resolved temporal and spatial air pollutant emission inventory for the Pearl River Delta region, China and its uncertainty assessment, Atmospheric Environment, 43, 5112-5122, 10.1016/j.atmosenv.2009.04.060, 2009.

Zhou, J., Murano, K., Kohno, N., Sakamoto, Y., and Kajii, Y.: Real-time quantification of the total HO2 reactivity of ambient air and HO2 uptake kinetics onto ambient aerosols in Kyoto (Japan), Atmospheric Environment, 223, 10.1016/j.atmosenv.2020.117189, 2020.

Zhou, J., Sato, K., Bai, Y., Fukusaki, Y., Kousa, Y., Ramasamy, S., Takami, A., Yoshino, A., Nakayama, T., Sadanaga, Y., Nakashima, Y., Li, J., Murano, K., Kohno, N., Sakamoto, Y., and Kajii, Y.: Kinetics and impacting factors of HO_2 uptake onto submicron atmospheric aerosols during the 2019 Air QUAlity Study (AQUAS) in Yokohama, Japan, Atmospheric Chemistry and Physics, 21, 12243-12260, 10.5194/acp-21-12243-2021, 2021.

Zhu, L., Jacob, D. J., Eastham, S. D., Sulprizio, M. P., Wang, X., Sherwen, T., Evans, M. J., Chen, Q. J., Alexander, B., Koenig, T. K., Volkamer, R., Huey, L. G., Le Breton, M., Bannan, T. J., and Percival, C. J.: Effect of sea salt aerosol on tropospheric bromine chemistry, Atmospheric Chemistry and Physics, 19, 6497-6507, 10.5194/acp-19-6497-2019, 2019.

Ziska, F., Quack, B., Abrahamsson, K., Archer, S. D., Atlas, E., Bell, T., Butler, J. H., Carpenter, L. J., Jones, C. E., Harris, N. R. P., Hepach, H., Heumann, K. G., Hughes, C., Kuss, J., Kruger, K., Liss, P., Moore, R. M., Orlikowska, A., Raimund, S., Reeves, C. E., Reifenhauser, W., Robinson, A. D., Schall, C., Tanhua, T., Tegtmeier, S., Turner, S., Wang, L., Wallace, D., Williams, J., Yamamoto, H., Yvon-Lewis, S., and Yokouchi, Y.: Global sea-to-air flux climatology for bromoform, dibromomethane and methyl iodide, Atmospheric Chemistry and Physics, 13, 8915-8934, 10.5194/acp-13-8915-2013, 2013.